IUBAT Review—A Multidisciplinary Academic Journal, 6(2): 41-76
https://doi.org/10.3329/iubatr.v6i2.71308

Water Dispersible Colloidal Metal and Metal Oxide Nanoparticles Synthesis for Agarwood Inoculation: A Review

Dr. Md. Jahidul Islam[1*], Md. Kawsar Uddin[2], Dr. Mohammad Jakir Hossain[3]

[1]Department of Chemistry, International University of Business Agriculture and Technology (IUBAT), Dhaka 1230, Bangladesh.
[2]Department of English and Modern Languages, International University of Business Agriculture and Technology (IUBAT), Dhaka 1230, Bangladesh.
[3]BFRI, Bangladesh Forest Research Institute.

Keywords:
Agarwood, Inoculation, Water soluble Nanoparticle, Noble metal nanoparticles, Metal oxide nanoparticles, Biotechnology.

Abstract
Agarwood is one of the most expensive natural products, produced from Aquilaria Spp. These plants produce agar resin through mechanical, biological, or chemical stress. Besides these, the particles having size in the range of 1-100 nm, are known as nanoparticles, have ultra-high surface area and surface plasmon resonance, can create stress on living plants when incorporated into the plant body. Adopting this concept, we intend to produce agarwood by inoculating water-dispersible metal/metal oxide nanoparticles. Therefore, we aim to synthesize water-dispersible four noble metals (Au, Ag, Pt, Pd) and five metal oxides (Fe_3O_4, TiO_2, SnO_2, MnO_2, CuO) nanoparticles in aqueous colloidal states for application in biotechnology, considering the facile synthetic routes, readily available and inexpensive precursors, and stability of the products under normal laboratory conditions for an extended period, utilizing the synthesis methods of precipitation of metal/metal oxide nanoparticles from an aqueous solution, microwave and ultrasound-assisted rapid heating methods, sol-gel methods, and surfactant-assisted microemulsion methods. We believe that by applying any of these methods, water-dispersible, long-lasting colloidal metal/metal oxide nanoparticles can be synthesized using a simple laboratory setup, without the need for sophisticated tools or instruments.

1. Introduction

Nanoparticles are usually defined as particles with sizes ranging from 1 to 100 nanometers (nm), and their dimensions can be extended up to 1-1000 nm (Hossain *et al.*, 2013). The typical diameter of a carbon atom is 0.098 nm, actinium is 0.215 nm, and a single water molecule is 0.27 nm. Particles smaller than 1 nm are commonly referred to as atomicclusters, for example, the Au_{15} cluster with a molecular diameter of 0.86 nm.

*Corresponding author's E-mail address: jahidul.che@iubat.edu
Article received:August 29, 2023,Revised and accepted:November 06, 2023, Published:December 31, 2023

If nanoparticles exist as separate entities in a liquid medium, they are referred to as a colloid, which is a physical mixture where the solute particles ranging in diameter from 1-1000 nm are evenly dispersed in the solvent without precipitating out. Due to the ultra-small size of nanoparticles, their physical, chemical, optical, and electrical properties differ from those of bulk materials. The confinement of electrons within nanoparticles provides a powerful means to manipulate the electronic, optical, and magnetic properties of nanomaterials (Logothetidis, 2011).

Since nanoparticles are much smaller than the wavelengths of visible light (400-700 nm), they cannot be seen with ordinary optical microscopes. Specialized microscopes such as Transmission Electron Microscopy (TEM) and Scanning Electron Microscopy (SEM) are required. In addition to these microscopes, common instruments used for nanoparticle characterization include UV-Visible Spectroscopy, Inductively Coupled Plasma Mass Spectrometry (ICP-MS), Dark Field Microscopy, Zeta Potential Analyzer, Aerodynamic Particle Sizer (APS), Matrix-Assisted Laser Desorption/Ionization Mass Spectrometry (MALDI-MS), Dynamic Light Scattering (DLS), and Scanning Mobility Particle Sizer (SMPS) (Titus *et al.*, 2019).

One of the most important parameters of metal nanoparticles is the localized surface plasmon resonance, which refers to collective electron charge oscillations in metallic nanoparticles that are excited by light. This phenomenon causes characteristic optical color variations depending on the size, shape, and nature of the metals. Metal nanoparticles with surface plasmon resonance properties are widely used in biotechnology. For example, Amendola *et al.* reported the use of Au nanoparticles based on their surface plasmon resonance properties (Amendola *et al.*, 2017). Another important parameter of nanoparticles is their high surface area to volume ratio (Lai *et al.*, 2012). Due to this exceptional characteristic, nanoparticles are highly vulnerable to aggregation and further reactions. Nanoparticles can be classified into different types based on their constituent materials (Bhatia, 2016). The names of nanoparticles are derived from the constituents of the particles. Common forms of nanoparticles include metal nanoparticles such as Au, Ag, Pt, Pd, and Os; metal oxide nanoparticles such as Fe_3O_4, TiO_2, ZnO, and Al_2O_3; metal sulfide/selenide nanoparticles such as ZnS and CdSe quantum dots; organic nanoparticles such as dendrimers, micelles, and microemulsions; silica nanoparticles; and carbon nanoparticles such as carbon dots, carbon nanotubes, and fullerenes.

1.2 Impact of Nanoparticles in Biotechnology

Nowadays, nanoparticles are playing an outstanding role in many scientific sectors, thanks to their extraordinary chemical, physical, and electrical properties (Matsui, 2005). In the field of biotechnology, various types of nanoparticles are being extensively used (Elaissari, 2008). Nanoparticles not only have significant

applications in medical science but also contribute to other sectors, such as increasing agricultural crop production (Khan *et al.*, 2019).

In this paragraph, we briefly mention the applications of metal nanoparticles in the field of biotechnology. West *et al. (2000)* reported the use of gold nanoparticles as detecting probes for nucleotides. Barrena *et al*. (2009) evaluated the ecotoxicity of gold nanoparticles as model nanoparticles in Lactucasativa and Cucumis sativus and found an improvement in seed germination. It is also discovered that silver nanoparticles with a size of 6 nm effectively suppress the proliferation of human leukemic cells (Qingzhi *et al.*, 2012). Researchers found that silver nanoparticles inhibit the seed germination of Carex, Juncus, lobelia, panicum, phytolacca, and Scirpus plants (Yin *et al*., 2012). Ling-Na *et al.* (2014) reported that platinum nanoparticles act as signal transducers to develop a colorimetric assay for the direct detection of cancer cells. Rahman *et al.* (2020) found a toxic effect of Pt NPs on *Peperomia pellucid* crops. The use of palladium as a chemical tool, similar to gold and silver, for biomedical applications (Yaqoob *et al.*, 2020). Battke *et al.* (2008) reported the abiotic stress caused by palladium nanoparticles and the shrinkage of foliate in barley plants.

After describing the use of metal nanoparticles in the field of biotechnology, we now briefly discuss the potential and prevailing use of selected metal oxides in this arena. Lai *et al.* (2018) reported the effectiveness of iron oxide (Fe_3O_4) nanoparticles for bone marrow engineering applications. Junli et al. found the effects of ferromagnetic iron oxide nanoparticles on *Zeya* mays (Junli *et al.*, 2016). Jung-wook *et al.* (2007) reported the photocatalytic effects of titanium dioxide (TiO_2) nanoparticles on skin cancer cells. It is reported that TiO_2 nanoparticles inhibit root and shoot development and decrease plant biomass in tobacco (Zhang *et al.*, 2019). Khursheed *et al.* (2020) reported the potential use of copper oxide (CuO) nanoparticles in human breast carcinoma cells and their toxicity against *Aspergillus flavus*. DNA damage was found by Donald *et al.* (2012) in *Raphanus sativus*, *Lolium perenne*, and *Lolium rigidum* due to the treatment with 100 nm scale CuO nanoparticles. Preethy *et al.* (2014) reported the reactivity of manganese dioxide (MnO_2) nanoparticles towards peroxides for regulating the tumor microenvironment. Shakeel *et al.* (2022) found a significant increase in plant growth, photosynthetic pigments, and non-enzymatic antioxidant activity in cowpea due to the treatment with MnO_2 nanoparticles.

Vittori *et al.* (2015) found detrimental effects of tin dioxide (SnO_2) nanoparticles on potato plant growth. In addition, Khan *et al.* (2019) summarized the effects of various metal and metal oxide nanoparticles on different agricultural crops. They cited silver (Ag), gold (Au), iron oxide (Fe_3O_4), copper oxide (CuO), zinc oxide (ZnO), aluminum oxide (Al_2O_3), cerium oxide (CeO_2), titanium dioxide (TiO_2), and silicon dioxide (SiO_2) nanoparticles in the size range of 2 to 100 nm,

which can affect plant growth and inhibition depending on the concentration ranging from 0.01 to 1000 mg/L.

From the above mentioned refence, it makes a clear sense that different types of nanoparticles perturb the metabolic system of the plants body. We believe, these nanoparticles will also create some interaction with the agarwood tree and change the secondary metabolism which will consequently trigger the agarwood formation.

1.3 Nanoparticles and Agarwood

1.3.1 Current Scenario of Agarwood Research

Agarwood is the non-timber resinous part of *Aquilaria Spp*. This wood is one of the most expensive botanical products in the world. The price of top-grade agarwood is US$100,000/Kg, and the oil is priced at US$40,500/Litre (Thompson *et al.*, 2022). The high price of this product is attributed to its diverse uses in medicine, Ayurveda, aphrodisiacs, incense, and fragrance (Tan *et al.*, 2019). The formation of agarwood is associated with biotic or abiotic stress on agar trees. Agarwood is not produced by plants unless they are injured by natural or artificial disasters such as cyclones, droughts, excessive rainfall, log breakage, animal attacks, microbial infestations like bacteria, fungi, algae, or insect attacks. When trees experience sickness or stress, they trigger their defense mechanisms, leading to the biosynthesis of agar resin.

1.3.2 Artificial Inoculation of Agarwood

The formation of agar resin inside the tree is associated with the activation of various secondary metabolic pathways, such as the hydrogen peroxide pathway, jasmonic acid pathway, salicylic acid pathway, and the production of reactive oxygen species. Agar resin is essentially a chemical combination of different types of 367 sesquiterpenoids and phenylethyl chromone derivatives, which are biosynthesized inside the tree under stress by secondary metabolism (Gao *et al.*, 2019). Therefore, the main cause of agar resin formation is injury and the tree's survival response. These counterbalancing activities eventually lead to the deposition of agar resin. Healthy trees do not produce agar resin even in their long lifespan of 100 years. In natural agarwood gardens, only around 2or 10percent of trees may coincidentally contain agar resin by the age of 30 years.

Since agar trees produce agar resin only in response to injury, various traditional artificial injury systems are practiced, such as mechanical nailing, burning, chisel drilling, partial trunk pruning, and debarking (Tan *et al.*, 2019). However, these mechanical approaches are somewhat unscientific, labor-intensive, and time-consuming. Therefore, more scientific approaches are currently being explored and tested.

1.3.3 Agarwood Production by Chemical Approaches

Using a microbiological approach, fungus is cultured and introduced into the agar tree, which locally injures the tree and produces top-grade agar resin in a specific area (Tan *et al.*, 2019). Various chemical and biochemical approaches have also been attempted, such as the CA kit by Blanchet (Blanchette & Chowdhury, 2009), Agar wit by Chinese Liu (Wei *et al.*, 2010; Wei *et al.*, 2012; Yangyang *et al.*, 2013), and Agar bit by Chinese Lin (Zeqing *et al.*, 2020). The CA kit works in a limited, localized area of the plant body, while Agar wit operates based on water transpiration, dispersing throughout the entire tree. As a result, agar deposition occurs in 3 to 6 months throughout the tree. However, the solution disperses within a few hours due to the plant's transpiration pull, followed by the activation of the defense system. These agar kits consist of a combination of phytohormones and inorganic salts. Agar wit, for example, utilizes methyl jasmonate, salicylic acid, and inorganic salts such as sodium chloride, iron chloride, iron sulfate, potassium chloride, hydrogen peroxide, and others (Wei *et al.*, 2010; Wei *et al.*, 2012; Yangyang *et al.*, 2013). In some cases, individual chemicals such as NaCl and formic acid are also being used as inducers (Tan *et al.*, 2019).

1.3.4 Agarwood Present Status: Perspective Bangladesh

Indonesia is the leading country in terms of agarwood production and export. Other countries engaged in the agarwood business include Malaysia, China, India, Philippines, Myanmar, Cambodia, and Laos. The main importers, or consumers, are primarily from the Middle East. The annual global business for agarwood exceeds US$32 billion. From 2000 to 2020, Indonesia exported 16 million kg of agarwood products, while Bangladesh exported only 1.9 million kg. However, the good news is that in Bangladesh, there are over 30,000 hectares of manmade agarwood gardens (Thompson *et al.*, 2022) and over 60 million agar trees. The climate in our country is suitable for agarwood tree cultivation. Different chemical inocula have been tested for agarwood species in Bangladesh for accelerating agarwood production by artificially. According to most of the reports, either the agarwood trees died or no agar resin formation was observed. The exact reasons are still unexplored, but it is possible that over-dosing or differences in agarwood species compared to those used in trials in other countries are contributing factors. Therefore, there is a demand in our situation for a suitable kit formulation based on chemicals to produce agarwood.

1.3.5 Nanoparticles Inoculation for Agarwood

Nanoparticles have both positive and negative effects on growth systems, photosynthesis regulation, secondary metabolism regulation, reactive oxygen species generation, free radical generation, genetic transmutation, and chromosomal aberration (Landa, 2021; Rahmawati *et al.*, 2022). As mentioned in section 1.2, nanoparticles have been observed to have various effects on different plants. Considering these effects, it can be hypothesized that nanoparticles can also trigger the defense system of agar trees and ultimately lead to agar resin production through nanoparticles inoculation. A feasibility study was conducted at BFRI (Jakir *et al.*,

2020), where it was discovered that iron oxide nanoparticles can trigger agarwood formation, resulting in agar resin production within three months of inoculation. These findings present the possibility of using nano-inducers to accelerate agarwood production in a shorter time frame and at a lower labor cost. Consequently, we are currently working on synthesizing different types of water-soluble metal and metal oxide nanoparticles to be inoculated into agarwood trees for agar resin formation.

Our objective is to inoculate the synthesized nanoparticles into agarwood plants to expedite the artificial formation of agar resin. Our main concern lies in the synthesis and stability of nanoparticles in an aqueous medium, as metal and metal oxide nanoparticles are typically hydrophobic and insoluble in water. Difficulties arise in preventing aggregation, as well as controlling the size and shape of the nanoparticles. To address these challenges, we have compiled a review article based on published reports that discuss the synthesis of colloidal nanoparticles in aqueous media. This compilation is expected to serve as a pioneering work in the field of nanoparticles synthesis in aqueous colloidal systems. Figure 1 shows the schematic diagram of producing of agar resin by inoculating nanoparticle in living agarwood plant.

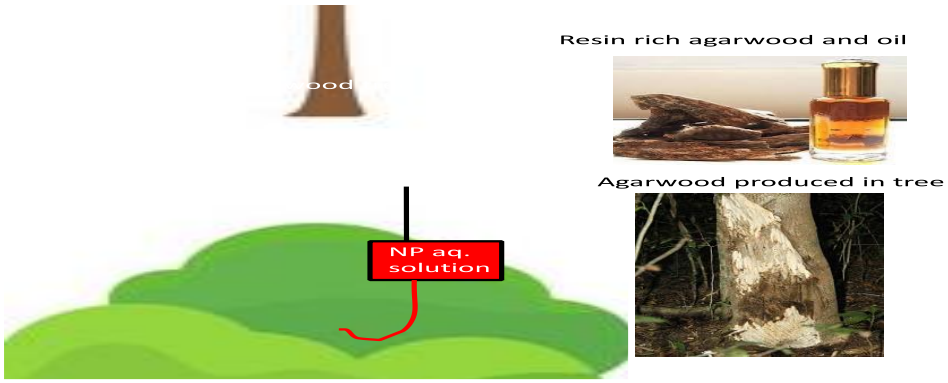

Figure 1: Agarwood production by nanoparticle (NP) inoculation

1.3.6 Accumulation and Transportation of Nanoparticles inside the Plant

The foremost criterion for applying nanoparticles to plants is their water solubility, as the dispersal of minerals inside the plant is primarily governed by the transpiration pull of water (Khan *et al.*, 2010; Wei *et al.*, 2019; Wei *et al.*, 2012; Yangyang *et al.*, 2013). Nanoparticle are hydrophobic in nature. Plant body are also hydrophobic. So, the hydrophobic nature of the plant body and nanoparticle enables their electrostatic interaction, which may contribute and facilitate the movement of the nanoparticle inside the plant. Plants have various mechanisms that allow the entry of nanoparticles up to 1000 nm in size (Khan *et al.*, 2019). One such mechanism is the presence of aquaporins, which are 1 nm diameter water channels

located within the plant membrane. Aquaporins mainly regulate the water and mineral concentrations in the plant, enabling the acceptance of particles up to 1 nm in size (Hill, 1994). Additionally, the cell wall of plants contains pores ranging from 5 to 10 nm in diameter and several micrometers in length (Wyman, 2013), allowing particles within the 1-10 nm size range to pass through. The accumulation mechanism of different size of nanoparticles inside the plant is shown in the figure 2.

Nanoparticles larger than 10 nm can enter plant cells through another route known as plasmodesmata, which are cylindrical microchannels, approximately 40 nm in length, facilitating the entry of particles larger than 40 nm (Lin & Xing, 2008). For particles larger than 40 nm, plants employ an endocytosis mechanism (Decuzzi *et al.*, 2007; Zhang *et al.*, 2015). In this process, when foreign particles come into contact with the cell wall, the plant cell forms intracellular vesicles that engulf the target particles. The diameter of the formed vesicles depends on the size of the incoming particles, and through endocytosis, particles up to 1000 nm in size can be accumulated inside the plants (McNeil, 1984; Pérez-de-Luque, 2017; Swanson, 2008). Although even micron-sized particles can be permitted inside plants, the most suitable sizes for accumulation and further transportation of particles inside plants are typically in the range of 5-20 nm. Of course, we have to consider the points that, the small size nanoparticle easily can move from one position to another postion inside the plant, within very short time, but for movement of big particles, it must need much time and stronger transpiration pull through the zigzag microchannel of the plant cell. For the transportation of the different types of minerals and water inside the plant cell, tree use vascular bundle which is consist of xylem and phloem tissues. The upward direction transition of material inside the plant cell is governed by transpiration pull of water and pass trough xylem tissue. The downward movement of the particle and chemicals are regulated by the gravitational force and pass through the phloem tissue to the different part of the plant body. Any particle come inside the plant body from terrestrial and aerial parts by stomata then pass through the trichome and cuticle layers for incorporation into the plant body.

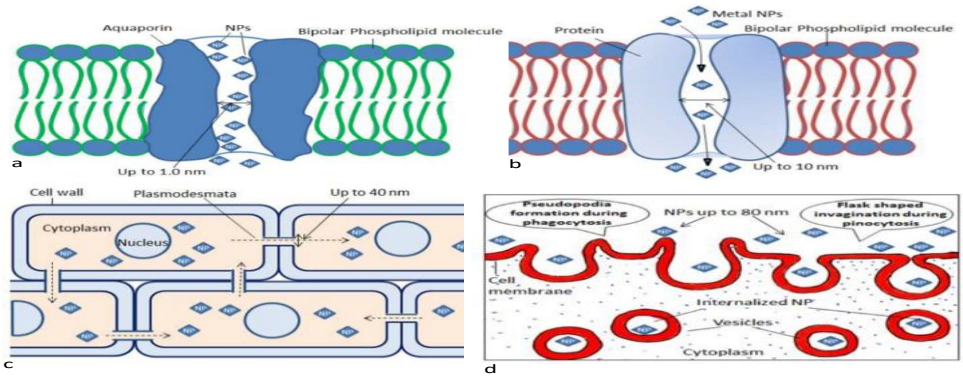

Figure 2: Accumulation of different size of nanoparticle by living plant.

Accumulation of - (a) 1 nm size NP by aquaporin (b) 10 nm size NP by cell membrane (c) 40 nm size NP by cell plasmodesmata (d) 80 nm size NP by pinocytosis. Figure is reprinted with permission from Reference (Khan *et al.*, 2019) Copyright 2023 by John Wiley & Sons.

1.4 Selection Criteria for Choosing Nanoparticles

When compiling the protocols for synthesizing water-dispersible nanoparticles, several points are considered. These include a simple procedure, stable precursors, ease of handling, product size in the range of 20 nm or close to it, stability in the aqueous phase for a long time, and prevention of aggregation.

A simple procedure refers to the absence of sophisticated instruments or strictly controlled environments, such as a glove box or extremely hot/cold temperatures that would be difficult to maintain in an open environment for an extended period. Stable precursors are those that can be safely stored in an open environment without causing any chemical hazards.

Ease of handling means that no sophisticated personal protection or attire is required. This is important when synthesizing nanoparticles on a large scale for applications in open environments, such as infusion into plants or animal cells, where it is not possible to control the internal environment of biological cells.

Nanoparticles can exist in different morphological states with various shapes, including spherical, circular, cubic, square, rod, pyramid, hexagon, octahedron, plate, icosahedron, and more. The size, shape, and stability of synthesized nanoparticles depend on various factors such as the nature and concentration of initial precursors, mole ratio, solvent nature, and polarity, p^H, and temperature.

1.5 Growth Mechanism of Nanoparticles

The growth mechanism of nanoparticles can be explained using the concept developed by Younan, based on the LaMer theory (LaMer & Dinegar, 1950; Xiong *et al.*, 2009). According to this explanation, in the growth of metal nanoparticles, atomization occurs through the action of a suitable reducing agent that converts metal ions from their salt states into free atoms. When the concentration of these free atoms surpasses the supersaturation level, nucleation begins and continues until the concentration falls below this level. These nuclei act as seeds for further nanoparticle growth. If the concentration remains sufficient, the nucleus continues to grow with the addition of more atoms to it. In this case, the rate-determining step is the nucleation of free atoms. Ciacchi et al. provide an alternative mechanism where atomization is not necessary to initiate nanoparticle nucleation (Ciacchi *et al.*, 2003). Instead, existing clusters of atoms in the precursor salt act as seeds for nucleation. Khan *et al.* (2019) demonstrate the stepwise reduction- nucleation-enlargementation- stabilization process based silver nanoparticle formation by using plant extract tyrosine as the reducing agent (figure 3).

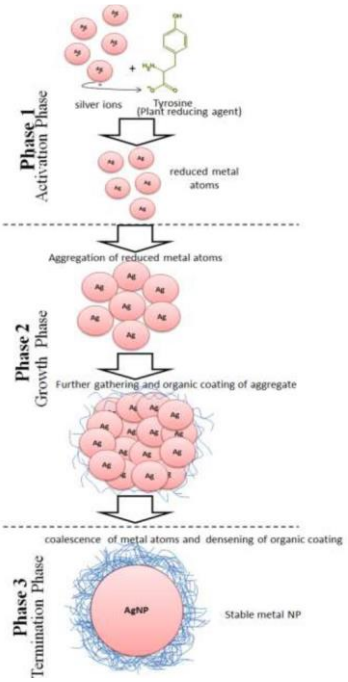

Figure 3: Growth mechanism of silver nanoparticles, reduction and stabilization by plant extract tyrosine.

The figure is reprinted with permission from references (Khan *et al.*, 2019) copyright 2000-2003 by John Wiley and Sons.

Stable metal nanoparticles are typically achievable for noble metals such as gold, platinum, silver, and palladium. These metals are generally unreactive or inert in their surrounding environments for extended periods. However, with special precautions, it is possible to synthesize nanoparticles of transition metals and other reactive metals. For transition metals, metal oxide nanoparticles are commonly preferred due to their improved stability in open environments rather than the pure metal nanoparticle. The growth mechanism of metal oxide nanoparticles differs somewhat from that of metal nanoparticles. Two explanations are proposed.

In one scenario, metalsalts convert to hydroxides, followed by condensation reactions and polymerization, ultimately leading to the generation of monomer oxides for nucleation (Oskam, 2006). In another explanation, metals are reduced by a suitable reducing agent, and then oxidation occurs through environmental oxygen. Once the concentration of these metal oxides reaches the supersaturation level, nucleation takes place and continues to grow following the mechanism observed for metal nanoparticles. For example, the growth of Fe_3O_4 occurs through the reduction of Fe^{2+}/Fe^{3+} to Fe^0, followed by oxidation using free O_2 from the environment.

2.1 Process of Synthesis of Metal and Metal Oxides Nanoparticles

The methodologies for synthesizing nanoparticles can be broadly categorized into two main approaches: top-down and bottom-up methods (Abid *et al.*, 2021). In top-down methods, larger bulk materials are transformed into smaller nano-sized particles, while in bottom-up methods, nanoparticles are grown from the atomic or molecular level. Among the top-down methods, notable approaches include ball milling, mechanochemical methods, laser ablation, and sputtering. The main bottom-up approaches include physical vapor deposition, chemical vapor deposition, spray pyrolysis, laser ablation, flame pyrolysis, biological methods induced by bacteria, fungi, yeast, algae, and plant extracts, sol-gel methods, chemical reduction, hydrothermal methods, and solvothermal methods. In this article, we will focus only on the wet chemical synthesis of nanoparticles in an aqueous medium, which does not require sophisticated equipment or techniques.

2.2 Common Wet Chemical Methods for Synthesis of Metal and Metal Oxides Nanoparticles

Depending on the intended application of the nanoparticles, various wet methods have been developed for preparing metal/metal oxide colloids. However, many of these methods have encountered issues such as polydisperse sizes, poorly defined shapes, and limited morphologies in the resulting samples. Currently, the most commonly applied methods for synthesizing nanoparticles in wet processes include precipitation methods, microwave irradiation, ultrasonic irradiation, chemical reduction, sol-gel methods, microemulsion, green synthesis, and others (Abid *et al.*, 2021). Different conditions are utilized for synthesizing and storing nanoparticles based on their intended applications. Our objective is to synthesize metal and metal oxide nanoparticles in an aqueous colloidal phase for use in biotechnology.

2.3 Synthesis of Metals from Aqueous Solutions by Precipitation

The common principle for producing metal nanoparticles involves the reduction of metal salts from their corresponding oxidized positive ions (Cushing *et al.*, 2004). Typically, reducing agents such as molecular hydrogen, alkaline metals and their borohydrides, and hydrazine hydrate or hydrazine chloride are employed. For the reduction to occur spontaneously, the free energy change of the reduction process must be favorable. This requires that the oxidation state of the metal ions be electrochemically positive, resulting in negative values for the final Gibbs free energy change. By adjusting the reaction p^H of the solution, it can be ensured that the change in net oxidation potentials is positive, ultimately yielding negative Gibbs energy values. When borohydride is used as the reducing agent, care must be taken to avoid the formation of metal borides. The electrochemical potential of borohydride and the oxidation states of the corresponding metal salts play a crucial role in this regard. The reduction potential of hydrazine in its pure or solvated states is -0.481 V (N_2H_4) or -0.23 V ($N_2H_5^+$), respectively. Therefore, metals with more positive reduction potentials can be reduced. The reduction potentials of most transition metal ions in the third and fourth periods lie within this range and are

applicable for reduction by hydrazine. Due to the instability of metal cations in aqueous solution, reduction potentials greater than -0.481 V are practically challenging. However, it is possible to synthesize metal nanoparticles by adjusting the p^H or other parameters of the reaction solution for the reduction of hydrazine in an aqueous solution.

The reduction of gold metal is achieved using weak reducing agents such as carboxylic acids or alcohols due to the higher oxidation potential of $AuCl_4^-$, (E°) +1.002 V. Therefore, various weak to strong reducing agents are suitable for reducing gold metals from aqueous solutions. Ten et al. reported the synthesis of silver, gold, and platinum nanoparticles reduced by citric acid using this concept (Tan *et al.,* 2003). These synthesized nanoparticles are stabilized by a capping ligand, and in many cases, the capping agent also acts as a reducing agent. Turkevich*et al.* reported similar wet chemical methods for the synthesis of citrate-stabilized gold nanoparticles, which have become widely used for teaching undergraduate students about nanoparticle synthesis in aqueous media using $HAuCl_4$ and sodium citrate as the precursor, reducing agent, and stabilizing agent (Turkevich *et al.,* 1951).

When thiol is used as a stabilizing agent for the synthesis of gold nanoparticles from $HAuCl_4$, a strong reducing agent should be employed instead of a mild reducing agent. This is because the complexation of $AuCl_4^-$with thiol is extremely stable. However, even under these conditions, if citric acid and thiol stabilizer are added simultaneously to the reaction solution, reduction of colloidal gold nanoparticles in the size range of 2-10 nm is possible by maintaining a high mole ratio of thiol to gold (Yonezawa *et al.,* 1997). For species with highly negative reduction potentials, strong reducing agents such as borohydride should be used instead of mild reducing agents. Borohydride is the appropriate reducing agent for metals such as Ni^{2+}, Co^{2+}, and Fe^{2+} (E°), with reduction potentials of -0.257 V, -0.28 V, and -0.447 V, respectively.

Thiol (bis (11-trimethylammonium decanoyl aminoethyl) disulphide dibromide or TADDD) is used as a stabilizer for silver nanoparticles with a size of 3.5 nm, which are synthesized using borohydride as the reducing agent (Yonezawa *et al.,* 2000). The excess borohydride is consumed during the reduction process, converting the disulphide to thiol. The resulting synthesized silver nanoparticles are soluble in slightly acidic water.

2.4 Synthesis of Metal Oxides Nanoparticles by Precipitation in Aqueous Medium

Precipitation is a chemical process in which solid formation occurs from a homogenous liquid solution under supersaturated conditions. The formation of metal oxide nanoparticles can occur in two ways. In one step, metal oxides are directly formed during the reaction (Cushing *et al.,* 2004). In the other way,

precursors or intermediates such as hydroxide, carbonate, or sulfate are formed initially, and the formation of the desired metal oxide nanoparticles is completed through calcination or heating. In this case, a stabilizer is often necessary to achieve the desired size nanoparticles. Otherwise, frequent agglomeration of the produced nanoparticles can degrade their monodispersity.

2.5 Nanoparticle Synthesis Using Microwave (MW)

Microwaves have the ability to rapidly and uniformly heat aqueous solutions, facilitating the rapid and monodisperse precipitation of nanoparticles with uniform sizes (Kumar *et al.*, 2020). The heating effect of microwaves on materials, solvents, and solutes causes the alignment of molecules with the applied electric field of the waves, resulting in an increase in frequency and the homogeneous generation of heat. This leads to the rapid formation of nanoparticles through nucleation. Pastoriza-Santos *et al*. (2002) utilized microwave heating to synthesize silver and gold nanoparticles, comparing the properties of these nanoparticles with those obtained through other heating methods, such as reflux, and found microwave synthesis to be a promising approach for nanoparticle synthesis.

2.6 Nanoparticle Synthesis by Ultrasonication

The ultrasonication method shares similarities with microwave-induced nanoparticle formation, but the underlying mechanism is different. Ultrasonic sound waves are converted into mechanical waves that generate high-frequency energy, creating thousands of heat cavities or bubbles. These microscopic heat cavities form within the reagents and experience a rapid increase in temperature, reaching several thousand degrees Celsius. The subsequent rapid cooling of the substance enables the quick formation of monodisperse nanoparticles. Suslick et al. synthesized metal nanoparticles (such as Fe and Co) using ultrasonication methods (Suslick *et al.*, 1991; Suslick *et al.*, 1996).

2.7 Sol-gel Chemistry for Nanoparticle Synthesis

Sol-gel processing is a commonly used wet chemical process for synthesizing metal and metal oxide nanoparticles. It typically involves five stages: hydrolysis, polycondensation, aging, drying, and thermal decomposition (Parashar *et al.*, 2020). In this method, the precursors used are alkoxides of the desired metal. These alkoxides undergo hydrolysis in water or alcohol through heating. The higher partial positive charge of the cation in most transition metals and silicon in their alkoxide form facilitates their easy hydrolysis. However, caution must be exercised with alkali and alkaline earth metals due to their exceptionally high charge, which can lead to explosive hydrolysis. The partial positive charges for Si, Ti, and Zr in their alkoxide states are +0.32, +0.63, and +0.74, respectively. Diao et al. synthesized magnesium nanoparticles by hydrolyzing $Mg(OEt)_2$ in a methanol-toluene mixed solvent (Diao *et al.*, 2002). Cao *et al.* (2002) demonstrated a template method using sol-gel processing to produce ZrO_2 nanoparticles.

2.8 Microemulsion System for Nanoparticles Synthesis

Microemulsion is defined as a thermodynamically stable liquid phase homogeneous mixture of oil and water, typically ranging in size from 10-100 nm. There are three types of microemulsion: oil in water (o/w), water in oil, and bicontinuous mixture. The ingredients of a microemulsion include water, water-soluble salts or ionic compounds, surfactant, and a long-tail organic layer that often contains a cosurfactant, which acts as an electrostatic charge repulsing agent to prevent agglomeration of microemulsion ingredients (Malik *et al.*, 2012).

To synthesize metal nanoparticles using a microemulsion, a microemulsion of soluble salts and another microemulsion of reducing agent are mixed together, resulting in the formation of a third microemulsion that contains transparent soluble metal nanoparticles. This method is similar to the aqueous phase precipitation of metal nanoparticles and is particularly favorable for metals with limited stability or solubility in the aqueous phase. For example, Boutonnet*et al*. synthesized 3 nm scale Pt nanoparticles by reacting H_2PtCl_6 with hydrazine in a water/pentaethyleneglycol dodecyl ether/hexane microemulsion (Boutonnet *et al.*, 1982).

Microemulsion is also used for synthesizing metal oxide nanoparticles using a similar approach to coprecipitation methods from aqueous solutions. Typically, a microemulsion of the target metal salts and another microemulsion of NH_4OH or NaOH are mixed vigorously, resulting in the formation of a third microemulsion with a transparent solution. This solution is then centrifuged, vacuum-dried, and heated if necessary. Using this method, CuO and SnO_2 nanoparticles can be produced. Nassar & Husein (2007) reported a synthetic route for water-soluble colloidal CuO nanoparticles using a water/dioctyl sulfosuccinate sodium salt/isooctane microemulsion system, starting from the reaction of $CuCl_2$ and NaOH.

2.9 Surface-derivatization of Nanoparticles

The solution process allows for the control of the size, shape, morphology, and stability of nanoparticles by adjusting the ratio of precursors to product, solvent ratio, temperature, and p^H.These interactions enable the tuning of desired properties for metal, metal oxides, and sulfides nanoparticles in a colloidal system. Freshly grown nanoparticles are typically highly reactive and have a high potential energy to react with additional atoms, leading to an increase in particle size. To achieve stable nanoparticles, the Van der Waals forces of interaction among the nanoparticles need to be controlled through proper complexation of the nanoparticles with solvents.

This complexation process involves the adsorption of solvent molecules onto the surface of the freshly grown nanoparticles, forming several layers. These multilayer solvents carry high electrostatic charges, resulting in repulsion between

them. As a result, the attraction among the nanoparticles decreases, leading to increased stability (Cushing *et al.*, 2004).

2.10 Selection Criteria of Surfactants

For controlling the size of the nanoparticle, surface passivation by proper surfactant is one of the most common practices. Surfactant are long chain organic molecule having positive and negative charge containing pole. Surfactants used in nanoparticle synthesis should be chemically inert in relation to the reactants and products involved. Typically, surfactants consist of a hydrophilic ion, which needs to be sufficiently stable to function effectively. For example, surfactants like CTAB (cetyltrimethylammonium bromide) and AOT (sodium bis(2-ethylhexyl) sulfosuccinate) are considered stable when mild oxidizing agents like hydrogen peroxide or mild reducing agents like hydrazine are used. However, they may not be suitable when strong reducing agents like borohydride or strong oxidizing agents like potassium permanganate are employed.

In the case of using CTAB as a stabilizer for the reduction of silver ions, it is important to be cautious about the precipitation of AgBr due to the presence of bromide ions in the surfactant. Similarly, when attempting to form $KMnF_3$, the presence of Na ions in AOT can interfere with the process, leading to the formation of $NaMnF_3$. Therefore, the selection of surfactants should consider their compatibility with the specific reactants and products to ensure optimal results (Agnoli *et al.*, 2001).

2.11 Common Surfactants for Stabilizing Metal and Metal Oxide Nanoparticles

Different types of surfactants are used based on the specific requirements of the chemical environment for nanoparticle synthesis. The commonly used anionic surfactants are Sodium dodecyl sulfate (SDS), Sodium dodecylbenzene sulfonate (SDBS), Sodium bis(2-ethylhexyl) sulfosuccinate (AOT); Cationic surfactants- Cetyltrimethylammonium bromide (CTAB), Dimethyldioctadecylammonium chloride (DDAC); Nonionic surfactants- Polyoxyethylenated alkylphenol, Polyoxyethylenated alcohol, Pentaethylene glycol dodecyl ether (PEGDE), and Triton X-100.

3. Synthesis Protocols of Metal/Metal Oxide Nanoparticles

In this section, we will discuss laboratory synthesis protocols for metal and metal oxide nanoparticles. We aim to provide at least three protocols for each species, focusing on avoiding multi-step synthesis whenever possible. However, if multi-step synthesis is necessary, we will also discuss those protocols and include information about ligand exchange processes. Additionally, we will discuss the size of the resulting metal/metal oxide nanoparticles and their stability in aqueous media.

3.1.1 Ag NPs Synthesis Protocol-1.

Raveendran *et al.* (2006) reported a green approach for the synthesis of Ag nanoparticles. According to this method, 25 mL 0.1 M D-glucose and 2 mL of 0.20% (w%) aqueous starch solution are sequentially poured into 10 mL 0.1 M $AgNO_3$ aqueous solution, then heat in a microwave oven for one minute. The average size of the synthesized Ag NPs is 6 nm, highly stable, and do not show any signs of aggregation even after storage for several months.

3.1.2 Ag NPs Synthesis Protocol-2

For synthesizing different colors of silver nanoparticles in the colloidal phase, Mendis *et al*. (2016). established a facile method. In this method, separate aqueous solutions of silver nitrate, $NaBH_4$, hydrazine sulfate, and trisodium citrate are mixed in a beaker, maintaining the mole ratios given below. For red - 5 mL, 1x 10^{-3} M: 20 mL, 4 x 10^{-3} M: 30 mL, 1 x 10^{-2} M: 20 mL, 2 x 10^{-3} M; For orange- 5 mL, 1 x 10^{-3} M: 20 mL, 4 x 10^{-3} M: 30 mL, 2 x 10^{-2} M: 20 mL, 2 x 10^{-3} M; Yellow- 5 mL, 1 x 10^{-3} M: 20 mL, 3 x 10^{-3} M: 30 mL, 1 x 10^{-2} M: 0 mL, 0 M; green- 5 mL, 1 x 10^{-3} M: 20 mL, 3 x 10^{-3} M: 30 mL, 1 x 10^{-2} M: 20 mL, 2 x 10^{-3} M; purple- 5 mL, 2 x 10^{-3} M: 20 mL, 4 x 10^{-3} M: 30 mL, 1 x 10^{-2} M: 20 mL, 2 x 10^{-3} M; blue- 5 mL, 2 x 10^{-3} M: 20 mL, 4 x 10^{-3} M: 30 mL, 1 x 10^{-2} M: 20 mL, 2 x 10^{-3} M respectively. In all cases, the solution needs to be stirred continuously for 10 minutes. The average size of the synthesized Ag NPs is 10 - 50 nm. Room temperature is suitable for the reaction conditions. The produced Ag NPs remain stable for 3 months without noticeable aggregation at 4°C. Results are shown in figure 4.

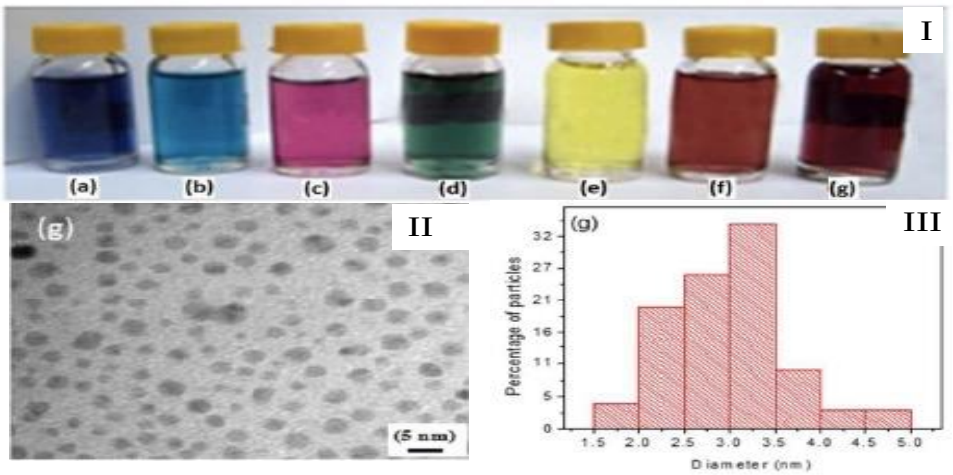

Figure 4: (I) Solution of different color silver nanoparticles produced by maintaing the different mole ratio of $AgNO_3$, $NaBH_4$, hydrazine sulfate, and Na_3Cit (II) TEM image of silver NP of sample g and (III) Dynamic light scattering data of sample g. The figure is reprinted with permission from Reference (Mendis *et al.*, 2016). Copyright 2023 Royal Society of Chemistry.

3.1.3 Ag NPs Synthesis Protocol-3

Doty *et al.* (2005) reported a synthesis protocol for colloidal Ag nanoparticles in the aqueous phase. According to this method, a freshly prepared aqueous solution of silver nitrate and trisodium citrate is mixed with continuous stirring. The volume of the solution is 200 mL, and the concentration of both precursors becomes 0.25 mM after mixing. Then, 6 mL of 10 mM sodium borohydride aqueous solution is suddenly added to the above mixture. The mixture is stirred for 30 minutes at room temperature and then left overnight at laboratory conditions without any stirring. The color of the solution turns yellow, indicating the formation of Ag colloidal nanoparticles. The average size of the synthesized Ag NPs is 8 nm. However, these nanoparticles are not stable for a long time. After 5 hours of synthesis, a thin film appears on the surface of the solution.

3.2.1 Au NPs Synthesis Protocol-1

Zeng and Jin (2015) reported a synthesis protocol for colloidal Au NPs in aqueous media. According to this process, 9.8 mg (0.025 mmol) of $HAuCl_4 \cdot H_2O$ is dissolved in 100 mL of nanopure water in a three-neck round-bottom flask under a nitrogen atmosphere. A 2.5 mL solution of trisodium citrate (38.3 mM) is added to the above solution all at once under reflux conditions, and the solution turns from yellow to red. The heating is continued for another 10 minutes, after which the solution is cooled to room temperature. Citrate-stabilized gold nanoparticles are purified by centrifugation. The average size of the Au nanoparticles is 18 nm, and they are sufficiently stable.

3.2.2 Au NPs Synthesis Protocol-2

One of the simplest one-pot syntheses for the stabilization of gold nanoparticles in the aqueous phase is reported by Nurakhmetova *et al.* (2020). In this method, 0.01 mM of $HAuCl_4$ (0.33 mL of 100 mg/mL solution) and 4 mL of KOH (0.5 M) are mixed with different types of polymers and refluxed at a desired temperature in a microwave reactor for 3-5 minutes.

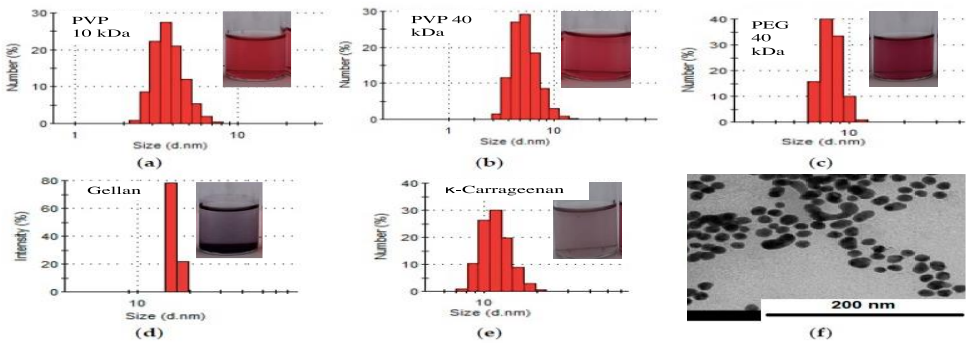

Figure 5: (a-e) Solution of different color gold nanoparticles stabilized by different polymers and their DLS data (f) TEM image of gold NP of sample b. Figure is reprinted with permission from Reference (Nurakhmetova *et al.*, 2020) Copyright 2023 Elsevier Science.

The optimum concentrations of the polymers are as follows (wt %): PVP - 4.0, gellan - 0.5, and pectin, welan, k-Carrageenan - 0.2. There are no noticeable changes observed in the size and shape of the nanoparticles if the reflux temperatures vary from 25°C to 100°C. Different sizes of nanoparticles are obtained by using different molecular weights of PVP. PVP MW 350 kDa results in NPs size of 25 nm; 40 kDa results in 8 nm; 10 kDa results in 4 nm, respectively. A color change from yellow to red/purple/colorless is observed during the reaction. Except for gellan, where monodispersed nanoparticles are obtained, in the case of other polymers, polydispersity is very common. The stability of the synthesized Au NPs in the presence of water-soluble polymers is 36 days. The results are shown in the figure 5.

3.2.3 Au NPs Synthesis Protocol-3

Doty *et al.* (2005) synthesized Au nanoparticles using a green approach. In this method, 40 µL of 0.1 M $HAuCl_4$ is mixed with 60 µL of 0.1 M aqueous D-glucose solution. The above solution is then mixed with an aqueous starch solution (0.2% w/w). Later, 15 µL of 1 M NaOH solution is added to the above transparent solution and stirred for 30 minutes. The reaction solution turns from yellow to red, indicating the formation of Au nanoparticles. The average size of the glucose/starch-stabilized Au nanoparticles is 6-10 nm, and they remain stable without noticeable aggregation for several months.

3.3.1 Pt NPs Synthesis Protocol-1

Water dispersible Platinum nanoparticle is synthesized by Bigall *et al.* (2008). According to this method, firstly 36 mL solution which contain $H_2PtCl_6 \cdot 6H_2O$ (0.2 w%), is poured into 464 mL boiling water.

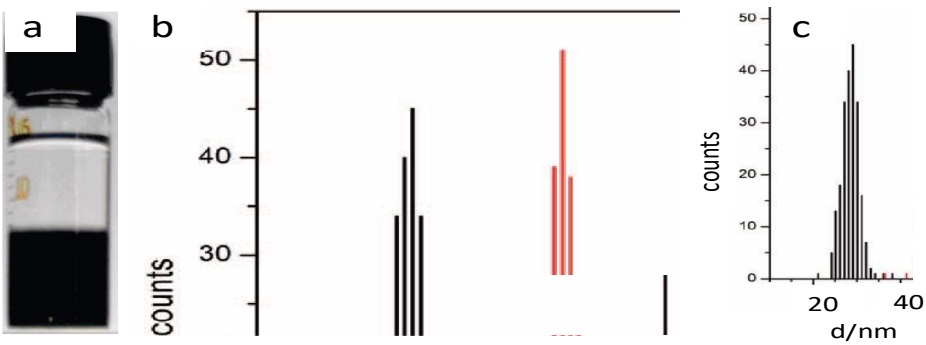

Figure 6: Citrate reduced and stabilized platinum nanoparticles (a) Solution (b) TEM image (c) DLS data. Figure is reprinted with permission from Reference (Bigall *et al.*, 2008) Copyright 2023 American Chemical Society.

Then a mixed solution of Na_3Cit (1%, w %) and citric acid (0.05%, w %) of 11 mL is poured into the above-mentioned boiling solution just after one minute. Half a minute later, another solution of $NaBH_4$, 5.5 mL, 0.08% (w%), which contain Na_3Cit (1%, w %) and citric acid (0.05%), is injected swiftly. Finally, the solution

is allowed to cool to room temperature. Average size of the citrate stabilized Pt nanoparticles is 5 nm (figure 6).

3.3.2 Pt NPs Synthesis Protocol-2

Bönnemann *et al.* (1996) reported a water-soluble Pt NPs synthesis protocol. In an oil bath at 145 °C, 0.104 g of $PtCl_4$ (0.31 mmol) was dissolved in 80 mL of distilled water in a 2-neck flask for reflux. 0.092 g (0.31 mmol) of dihydrocinchonidine dissolved in 7 mL of formic acid (0.1 N) was rapidly introduced to the above solution and heated for 10 minutes. The initial cloudy color converted to black within a few minutes. By following this process, 2.8 nm-sized, completely water-dispersible black powder of Pt NPs was obtained.

3.3.3 Pt NPs Synthesis Protocol-3

Xu and Yang (2008) reported a synthesis protocol for Pt nanoparticles. According to this method, 0.181 g of $H_2PtCl_6{\cdot}6H_2O$ and 1.0 g of sodium oleate are dissolved in 45 mL of distilled water. Then, 1.0 g of NaOH and 1.0 g of hexamethylenetetramine (HMT) are dissolved in the above solution. The mixture is heated to 100°C for 6 hours. The synthesized Pt NPs have an average size of 10 nm.

3.4.1 Pd NPs Synthesis Protocol-1

Xiong *et al.* (2007) reported a synthesis protocol for colloidal Pd nanoparticles in an aqueous medium. In their typical method, 5 mL of ethylene glycol (EG) is poured into a 25 mL three-neck flask, which is equipped with a condenser for reflux at 100°C in an open-air environment with constant magnetic stirring. At room temperature, 0.0486 g of Na_2PdCl_4 and 0.600 g of KBr are dissolved in 3 mL of water, and 0.0916 g of polyvinylpyrrolidone (PVP) in 3 mL of EG separately. The mole ratio of Pd: Br: PVP should be 1:30:15. The aforementioned two solutions are then injected in parallel into the refluxing flask using a two-channel syringe pump at a rate of 45 mL/h, and then refluxed for one hour at 100°C in an open-air environment.Upon completion of the heating, the product is collected by centrifugation and washed with acetone (once) and with ethanol (three times) to remove unreacted precursors of EG and PVP. By varying the reaction conditions (temperature) and the initial mole ratio of precursors, Pd nanoparticles of different shapes and sizes, typically around 10 nm, can be synthesized.

3.4.2 Pd NPs Synthesis Protocol-2

Antonio *et al.* (2010) reported synthesis protocol of colloidal Pd NPs in aqueous media. According to this method glucose, tetrabutylammonium hydroxide (TBAOH), and Pd-acetate are placed in a 1 mL gastight vail with screw cap, with maintaining the mole ratio of 0.25 mmol, 1.5 mmol, and 3 mmol respectively. During the reaction a little spacing of vial head helps to avoid the formation of droplets at the wall off the vail. The reaction mixture is refluxed at 40 - 90 ^{o}C for 6 h in the open environment. Synthesized Pd NPs average size are 15 nm, and colloidal solution remain quite stable.

3.4.3 Pd NPs Synthesis Protocol-3

A water-dispersible 3-8 nm scale Pd NPs synthesis protocol is reported by Xu and Yang (2008). According to their process, one solution of 0.026 g (0.147 mmol) of $PdCl_2$ in 5 mL (0.1%) of HCl, and another solution of 1.0 g of sodium oleate in 40 mL of water, are separately prepared by dissolution. Under vigorous stirring, the above two solutions are mixed with 1.0 g of hexamethylenetetramine (HMT) and kept for 10 minutes under the stirring condition. The resultant solution is visually lemon in color, and the p^H is around 9.

After heating at 100°C for 10 minutes, the solution turns black from a turbid color. After an additional 20 minutes of heating, the solution further darkens to black, and then it is allowed to cool to room temperature. The final p^H of the solution becomes 9.2, and the solution is precipitated by adding butanol and centrifugation. The resulting Pd NPs are in the range of 3 to 8 nm and remain stable for more than 6 months.

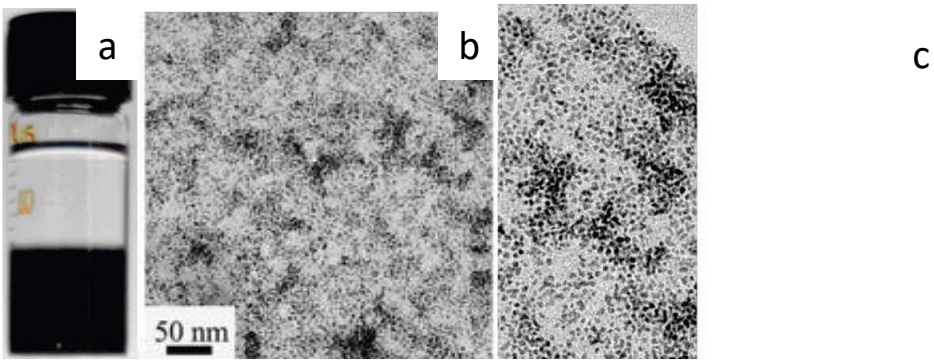

Figure 7: Hhexamethylenetetramine stabilized Palladium nanoparticles (a) Solution (b) TEM image (c) DLS data. Figure is reprinted with permission from Reference (Xu & Yang, 2008) Copyright 2023 American Chemical Society.

3.5.1 Fe_3O_4 NPs Synthesis Protocol-1

Dheyab *et al*. (2020) reported a simple and rapid synthesis and stabilization methods for Fe_3O_4 nanoparticles in aqueous phase. 50 mL NaOH solution is dropwise poured into nitrogen purged 180 mL aqueous solution of mixed oxidation state iron chloride salt $FeCl_2.4H_2O$ (2.5g), $FeCl_3.6H_2O$ (4.0g). The solution is maintained at 65 °C under magnetic stirring (650 rpm) for 10 minutes. 150 mL citric acid is added to this solution under the reaction condition and kept for more 10 minutes. As synthesized Fe_3O_4 NPs stabilized by citrate ion is collected by magnet and rinsed with distilled water and redispersed in water for further analysis. The size of citrate stabilized Fe_3O_4 NPs are 19 nm. Zeta potential values of the synthesized NPs are − 31.3 to − 45.3 mV, which indicates the higher repulsion among the nanoparticles and better stability. The results is shown in the figure 8.

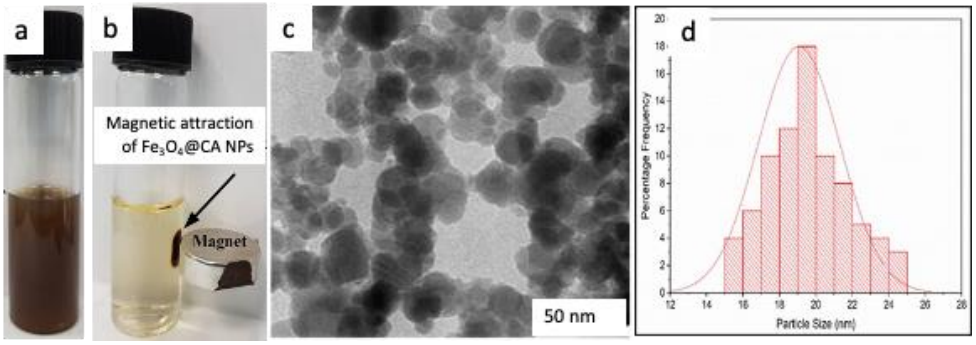

Figure 8: Citrate stabilized Fe_3O_4 nanoparticles (a-b) Solution (c) TEM image (d) DLS data. Figure is reprinted with permission from Reference (Dheyab *et al.*, 2020) Copyright 2023 Nature Elsevier.

3.5.2 Fe_3O_4 NPS Synthesis Protocol-2

Aslam *et al., (*2007) developed a methodology for the synthesis of Fe_3O_4 nanoparticles in water. Freshly prepared 100 mL of 10 mM $FeCl_2 \cdot 4H_2O$ aqueous solution is reduced at 85°C by 40 mM dodecyl amine. Although nanoparticle formation happens just after mixing the two solutions, even at room temperature, higher temperature is required for complete conversion. The as-synthesized nanoparticles are separated magnetically and washed with a small amount of acetone and deionized water for further characterization. The redispersed Fe_3O_4 nanoparticles in water are stable for more than one month without noticeable aggregation. TEM and DLS measurements published the nanoparticle size around 12 nm.

3.5.3 Fe_3O_4 NPs Synthesis Protocol-3

It is reported a water-dispersible Fe_3O_4 nanoparticles synthesis protocol (Lai *et al.*, 2004). 2.0 mmol of anhydride Iron (III) acetylacetonate is dissolved in 20 mL of nitrogen-purged and heated 2-pyrrolidone. The reaction is completed by refluxing the solution for 10 minutes. The precipitation is done by adding MeOH into the reaction solution at room temperature. A dark brown precipitate is washed with acetone. The water soluble Fe_3O_4 black powder is kept for further investigation. The average diameter of the synthesized nanoparticles is 5 nm. XPS results disclose that 370 molecules of 2-pyrrolidone form a layer on the surface of the 5 nm Fe_3O_4 NPs.

3.6.1 TiO_2 NPs Synthesis Protocol-1

Jung-wook *et al.* (2007) reported a water-dispersible titanium oxide nanoparticle synthesis protocol. According to this procedure, a solution of 0.5 mmol $TiCl_4$, 1 mmol oleic acid, and 6.5 mmol oleyl amine is refluxed at 270°C for 10 minutes. Using the size-selective precipitation method, the as synthesized TiO_2 nanoparticles are purified at room temperature. For surface modification, 20 mg of TiO_2

nanoparticles dispersed in 2 mL of toluene, are poured into a 1 mL solution of MeOH, containing 30 mg of DMSA (2,3-dimercaptosuccinic acid). After stirring the reaction solution for 24 hours, the surfactant-capped TiO_2 nanoparticles are purified by centrifugation. These DMSA coated TiO_2 nanoparticles are redispersed in water without any noticeable aggregation. The size of the colloidal titanium nanoparticles is 3x10 nm. These nanoparticles are stable in 250 mM aqueous brine solution and over a wide range of p^H (6-10).

3.6.2 TiO_2 NPs Synthesis Protocol-2

Yan *et al.* (2010) reported a facile synthetic route for colloidal phase TiO_2 nanoparticles. According to this method, under constant stirring, 3 mL of TBOT (tetra-n-butyl titanate) is dissolved in 6 mL of polyethylene glycol-400. Then, 1, 2, and 3 mL of 37% HCl are sequentially added to the above solution to produce TiO_2 nanoparticles in the form of anatase, mixed phase, and rutile, respectively. This transparent solution is heated at 80–150 °C for 10 hours in an autoclave.

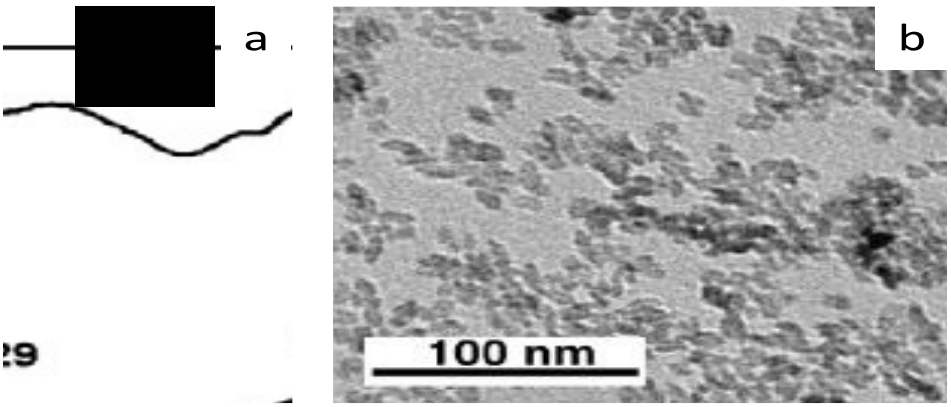

Figure 9: Polyethylene glycol (PEG-400) stabilized TiO2 nanoparticles (a) Solution (b) TEM image. Figure is reprinted with permission from Reference (Yan *et al.*, 2010) Copyright 2023 Elsevier.

The synthesized nanoparticles are purified by centrifugation at 12,000 rpm, washed with EtOH three times, and dried at 60°C for 12 hours.The as synthesized white-colored nanoparticles in all three forms are quite dispersible in water and EtOH. The size of the anatase TiO_2 NPs is around 10 nm, while the rutile TiO_2 NPs are basically nanorods with dimensions of 10 x 50 nm. The anatase form TiO_2 solution is the most stable, remaining stable for more than one month without noticeable aggregation. The result is shown in the figure 9.

3.6.3. TiO_2 NPs Synthesis Protocol-3

Zhang *et al.* (2016) reported polyethylene glycol (PEG) caped TiO_2 NPs synthesis protocol, using five different types of PEG 400, 2000, 4000, 6000 and 10000.

According to this method, white titanium alkoxide is produced by the reaction of 3 mL titanium n butoxide with 6 g of PEG under constant stirring at 65 ^{o}C. Drop by drop, one mL of hydrochloric acid is poured into the above solution. This transparent yellow solution is heated at 150 ^{o}C for 5 h in an autoclave. Yellowish orange color, TiO_2 nanoparticles are purified by centrifugation at 10,000 rpm, 3 times washed with EtOH, and vacuum dried at 50 ^{o}C for 24 hours. The size of the TiO_2 NPs caped by five different molecular weight of PEG 400, 2000, 4000, 6000 and 10000 are 76, 67, 61, 56, and 49 nm respectively. All the TiO_2 nanoparticles synthesized, using the different molecular weight of polyethylene glycol are well dispersed in water and ethanol and remain stable for long times, more than two months without noticeable aggregation.

3.7.1 CuO NPs Synthesis Protocol-1

Akhtar *et al.* (2019) reported a facile route for synthesizing water-dispersible tetraoctylammonium bromide (TOAB) surfactant-stabilized CuO nanoparticles. In this method, a 150 mL aqueous solution is prepared by dissolving 15.00 g of $CuSO_4{\cdot}5H_2O$ with 2.34 g of TOAB. The reaction solutions are refluxed at 65, 75, and 85 °C with constant shaking at 150 rpm for 15 minutes. Different sizes of nanoparticles are produced at different temperatures under these reaction conditions. For rapid precipitation, a 100 mL, 0.2 M NaOH aqueous solution is poured suddenly into the above solution. The as synthesized black CuO nanoparticles are washed with water and dried for further analysis. The average size of the nanoparticles ranges from 7 to 12 nm with a rod shape. No clear information about the stability of the nanoparticles is found, but they used the as synthesized CuO NPs in the aqueous medium for water disinfectant treatment without noticing any aggregation.

3.7.2 CuO NPs Synthesis Protocol-2

Nandanwar and Chakraborty (2012) reported a facile synthetic route for water-soluble colloidal CuO nanoparticles, using a water/oil microemulsion system. They used Triton X-100 as a surfactant for microemulsion preparation. A freshly prepared 0.1 M $CuCl_2$ aqueous solution is mixed with a 0.2 M Triton X-100 solution, prepared in cyclohexane, while maintaining the water/surfactant (w/s) mole ratio at four. The mixture is kept under constant stirring at 6500 rpm at room temperature for five minutes, or until the mixture becomes transparent. Similarly, using a 0.3 M NaOH aqueous solution in place of $CuCl_2$, a second reaction mixture is prepared. These two solutions are mixed under the same conditions and kept for 3 hours at room temperature. The produced CuO nanoparticles are washed with EtOH and acetone and collected by centrifugation. By following this protocol, it is possible to synthesize 15 nanometer scaled CuO nanoparticles.

3.7.3 CuO NPs Synthesis Protocol-3

Nassar and Husein (2007) reported a facile microemulsion-based synthetic route for copper oxide nanoparticles synthesis in an aqueous medium using AOT

(dioctylsulfosuccinate sodium salt) as the surfactant. A freshly prepared greenish aqueous solution of $CuCl_2$ is used as the source of copper. In their findings, the optimum concentration of the reaction conditions is 200 mM AOT in isooctane, 3.0 mM $CuCl_2$, 6.0 mM NaOH, with a mixing time of 3 hours, a temperature of 25°C, and stirring at 300 rpm. The mole ratio of $CuCl_2$: NaOH: AOT is 1:2:130, and the water: surfactant mole ratio is 5:1. A 20 mL AOT/isooctane microemulsion is prepared by dissolving $CuCl_2$ aqueous solution with stirring at room temperature. After observing the transparent microemulsion, the required NaOH solution is added and kept for 3 hours at room temperature under 300 rpm stirring. Using this method, 5 nm scale CuO nanoparticles are produced and remain stable for several months in the microemulsion. The result is shown in the figure 10.

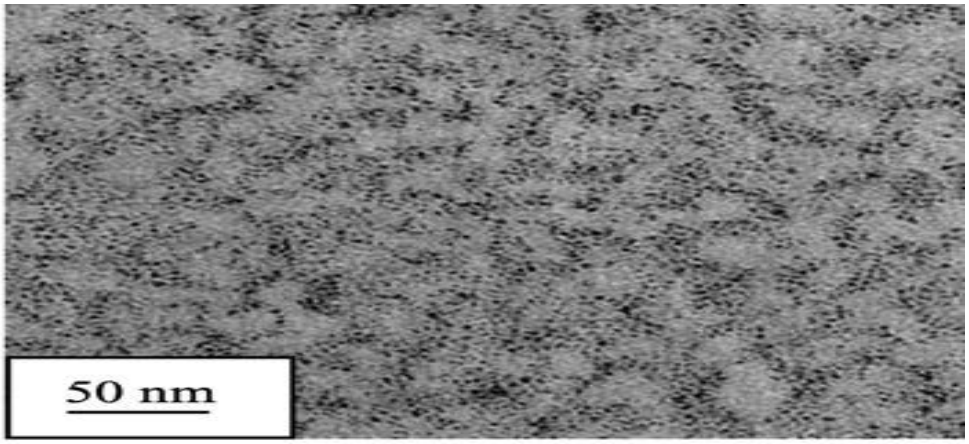

Figure 10: Wate: Dioctyl sulfosuccinate: Isooctane - microemulsion stabilized CuO nanoparticles TEM image. Figure is reprinted with permission from Reference (Nassar & Husein 2007) Copyright 2023 Elsevier.

3.8.1 MnO_2 NPs Synthesis Protocol-1

Islam and Rahman (2013) reported a facile synthetic route for producing water-soluble MnO_2 colloidal nanoparticles. In their report, they used three types of different reducing agents to produce MnO_2 from $KMnO_4$. The reducing agents are manganese sulfate ($MnSO_4$), formic acid (HCO_2H), and sodium thiosulfate ($Na_2S_2O_3$).

For the reduction of $KMnO_4$ by $MnSO_4$, 25 mL of 1.0 x 10^{-4} M $KMnO_4$ and 37.5 mL of 1.0 x 10^{-4} M $MnSO_4$ solution are mixed at room temperature under gentle stirring for 30 minutes, and then kept overnight at room temperature without any disturbance. A light yellow-colored homogeneous colloidal MnO_2 is observed.

For the reduction by HCO_2H and $Na_2S_2O_3$, the reaction conditions are the same, except for the initial mole ratios of the reactants. In the case of $Na_2S_2O_3$ as the reductant, 8 mL of 1.0 x 10^{-4} M $KMnO_4$ is mixed with 3 mL of 1.0 x 10^{-4} M $Na_2S_2O_3$,

and for HCO_2H as the reductant, 2 mL of 1.0 x 10^{-4} M $KMnO_4$ is mixed with 3 mL of 1.0 x 10^{-4} M HCO_2H.

In this report, there is no evidence about the size of the synthesized nanoparticles, but they showed characteristic evidence of 390 nm UV-vis spectrum peaks in all the cases, which confirmed the existence of MnO_2 in the solutions. There is no noticeable agglomeration observed in any of the colloids, even after months of waiting, which indicates the good chemical stability of the colloidal solution.

3.8.2 MnO_2 NP Synthesis Protocol-2

Khan *et al.* (2010) reported a colloidal MnO_2 synthesis route in the aqueous phase, using Cysteine and Methionine as the reducing agents. According to this procedure, 5 mL of 1.0 x 10^{-2} M $KMnO_4$ and 15 mL of 1.0 x 10^{-2} M Methionine are mixed and shaken for 2-3 minutes. Before shaking the solution, the total volume of the solution should be diluted to 50 mL by adding an additional 30 mL of water to the reaction solution. The characteristic purple color of the permanganate solution turns yellow-brown due to the reduction, implying the formation of manganese dioxide. In the case of Cysteine-reduced MnO_2 preparation, a brown-colored precipitate is immediately observed after mixing 5 mL of 1.0 x 10^{-2} M $KMnO_4$ and 30 mL of 1.0 x 10^{-2} M Cysteine in a reaction vial. The produced sample is washed with water and redispersed in water. The samples prepared using this procedure remain stable for several months, and the average particle size lies between 2-7 nm.

3.8.3 MnO_2 NPs Synthesis Protocol-3

Le *et al.* (2019) reported colloidal MnO_2 nanoparticle synthesis in an aqueous medium using a mixed reducing agent of hydrogen peroxide and polyvinyl alcohol (PVA). According to this procedure, 6 mL of 0.5 mol/L $KMnO_4$ is diluted to 100 mL with a mixed solvent, water: EtOH; 1:1, v/v. Under constant stirring conditions, a 10% hydrogen peroxide and PVA solution are poured into the above solution. Immediately, brown-colored precipitation of MnO_2 nanoparticles starts, just after mixing. Using hexane as the anti-solvent, the produced MnO_2 nanoparticles are precipitated out for further characterization. The average particle size of the produced MnO_2 nanoparticles is around 50 nm. They used the as-synthesized MnO_2 nanoparticles in an aqueous medium without notifying any aggregation.

3.9.1 SnO_2 NPs Synthesis Protocol-1

Lu *et al.* (2016) reported a simple method for producing thiourea-capped colloidal SnO_2 nanoparticles in an aqueous medium. According to this procedure, 0.9 g of stannous dichloride dihydrate salt and 0.3 g of thiourea are dissolved in 30 mL of water under constant stirring at room temperature. The cloudy suspension turns into a transparent yellow solution after 24 hours of continuous stirring, indicating the formation of SnO_2. The produced nanoparticles have a size of 3 nm and remain very stable at room temperature for a long time. The results is shown in the figure 11.

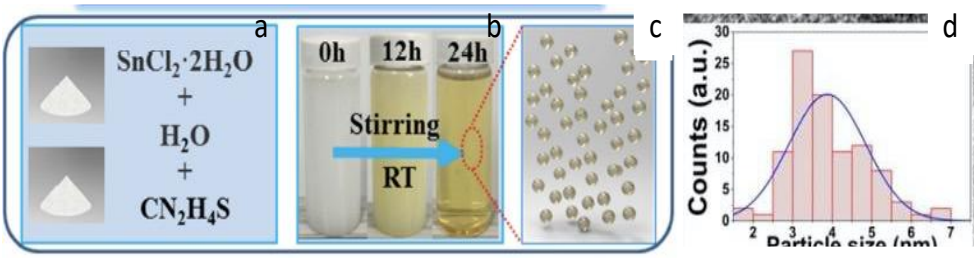

Figure 11: Thiourea capped SnO_2 nanoparticles (a) synthesis protocol (b) solution colour change with the progress of time (c) nanosized droplet (d) DLS data. Figure is reprinted with permission from Reference (Lu et *al.*, 2016) Copyright 2023 Elsevier.

3.9.2 SnO_2 NPs Synthesis Protocol-2

Suthakaran *et al.* (2019) reported a water-soluble colloidal SnO_2 nanoparticle synthesis protocol using three different types of stabilizers: polyethylene glycol (PEG) - a nonionic surfactant, Cetyl trimethylammonium bromide (CTAB) - a cationic surfactant, and sodium hexametaphosphate (SHMP) - an anionic surfactant. According to this protocol, 1.30 M of 50 mL NaOH solution is dropwise added to 0.26 M of 50 mL $SnCl_4 \cdot 5H_2$ O solution under constant stirring. After 45 minutes of stirring, when the solution turns transparent, 1 g of any one of the surfactants is added. The solution is kept stirring for another 30 minutes until it becomes transparent. This solution is incubated at 160 °C for 12 hours in an autoclave. The incubated solution is washed with water and ethanol at room temperature and finally dried in an oven at 100 °C for 6 hours. The nanoparticles sizes of SnO_2, stabilized by PEG, CTAB, and SHMP are 4.44 nm, 4.31 nm, and 3.33 nm, respectively.

3.9.3. SnO_2 NPs Synthesis Protocol-3

Sophie *et al.* (2002) reported water soluble SnO_2 nanoparticles synthesis protocol. According to this procedure, 1 g of tin isopropoxide is dissolve in 10 g of dry ethanol. Acetylacetone, (acacH) is added to the reaction mixture where the mole ratio of (acacH)/Sn is 5. Then (p-toluenesulfonic acid, PTSA) is added to the reaction solution under constant stirring for 2 hours by maintaing the ratio of PTSA/Sn is 0.4. This solution is sealed in a glass vial and kept for 24 hours at 60 ^oC using an oven. Optimum condition is water/Sn mole ratio is 10. The mean size of the SnO_2 nanoparticles is about 1–2 nm. The formed sols are stable at 4 ^oC for long time but convert to gel at room temperature after few weeks.

3.10. Overall View of Nanoparticle Synthesis Protocols

All the metal and metal oxide nanoparticle synthesis protocols in aqueous phase, for the application in agarwood inoculation are summarized in the table 1. Here we are drawing an overall view of nanoparticle synthesis protocols. In one of the protocols, Ag NPs were prepared from aqueous $AgNO_3$, glucose, and starch by microwave

heating within minutes. In the second protocol, different colors of silver nanoparticles were prepared by maintaining different initial mole ratios of silver nitrate, sodium borohydride, hydrazine sulfate, and sodium citrate. In the third protocol, silver NPs were prepared using citrate ion as a stabilizer. Gold NPs were prepared from chloroauric acid and sodium citrate just by reflux, following the first mentioned protocol. In the second protocol, Au NPs were prepared using different types of polymers as a reducing agent and stabilizer in an alkaline medium. Polyvinylpyrrolidone, gellan, welan, pectin, and k-carrageenan polymer stabilization allowed making 3-5 nm scale particles of Au NPs. In the third protocol, Au NPs were prepared using glucose and starch as a reducing agent from chloroauric acid as the precursor.

Platinum nanoparticles were prepared from chloroplatinic acid, sodium borohydride, and a sodium citrate/citric acid mixture by simple refluxion methods. In the second method of Pt nanoparticles synthesis, dihydrocinchonidine, formic acid, and platinum tetrachloride were refluxed at 145 ^{o}C and 2 nm scale particles were obtained. 10 nm scale Pt NPs were prepared in the third protocol from the reaction of chloroplatinic acid and hexamethylenetetraamine. Different shapes and sizes of Pd nanoparticles were prepared from the reaction of Na_2PdCl_4, KBr using sodium oleate, ethylene glycol, and polyvinylpyrrolidone as a stabilizer and reducing agent. In another method of Pd NPs synthesis, Pd acetate, glucose, and tetrabutylammonium hydroxide were refluxed at 90 ^{o}C, and 10 nm scale nanoparticles were obtained in 6 hours. In the third protocol, Pd NPs were synthesized from the reaction of $PdCl_2$ and HCl using Sodium Oleate, hexamethylenetetraamine as a reducing agent and stabilizer by simple heating at 100 ^{o}C for 10 minutes.

Table 1: Summary of the metal and metal oxide nanoparticle synthesis protocols in aqueous phase for the application in biotechnology

NPs protocols	Precursors	Size/nm	Stability	Reference
Ag NP protocol-1	$AgNO_3$, Glucose	6	months	60
Ag NP protocol-2	$AgNO_3$, $NaBH_4$, Hydrazine sulfate, Na_3Cit	10-50	months	61
Ag NP protocol-3	$AgNO_3$,Na_3Cit, $NaBH_4$	8	week	62
Au NP protocol-1	$HAuCl_4 \cdot H_2O$, Na_3Cit	18	-	63
Au NP protocol-2	$HAuCl_4$, KOH, polyvinylpyrrolidone (PVP), gellan, pectin, welan, k-Carrageenan	4-25	months	64
Au NP protocol-3	$HAuCl_4$, glucose, NaOH	10	months	62
Pt NP protocol-1	$H_2PtCl_6 \cdot 6H_2O$, Na_3Cit, citric acid, $NaBH_4$	5	-	65
Pt NP protocol-2	$PtCl_4$, dihydrocinchonidine, formic acid	3	-	66
Pt NP protocol-3	$H_2PtCl_6 \cdot 6H_2O$, sodium oleate, NaOH, hexamethylenetetramine	10	-	67
Pd NP protocol-1	Na_2PdCl_4, ethylene glycol, KBr, PVP	10	-	68

Pd NP protocol-2	Pd-acetate, tetrabutylammonium hydroxide	15	-	69
Pd NP protocol-3	$PdCl_2$, HCl, sodium oleate, hexamethylenetetramine	3-8	6	70
Fe_2O_3 NP protocol-1	$FeCl_2.4H_2O$, $FeCl_3.6H_2O$, NaOH	19	-	71
Fe_2O_3 NP protocol-2	$FeCl_2 \cdot 4H_2O$, dodecylamine	12	-	72
Fe_2O_3 NP protocol-3	Iron (III) acetylacetonate, 2-pyrrolidone	5	-	73
TiO_2 NP protocol-1	$TiCl_4$, oleic acid, oleyl amine, 2,3-dimercaptosuccinic acid	3x10	-	74
TiO_2 NP protocol-2	tetra-n-butyl titanate, polyethylene glycol-400, HCl	10x50	month	75
TiO_2 NP protocol-3	Ti- n butoxide, polyethylene glycol (PEG)	49-76	months	76
CuONP protocol-1	$CuSO_4 \cdot 5H_2O$, NaOH, tetraoctylammonium bromide	7-12	-	77
CuONP protocol-2	$CuCl_2$,Triton X-100, cyclohexane	15	-	78
CuONP protocol-3	$CuCl_2$, dioctylsulfosuccinate sodium salt, isooctane, NaOH	5	months	58
MnO_2 NP protocol-1	$KMnO_4$,$MnSO_4$, formic acid, $Na_2S_2O_3$	-	months	79
MnO_2 NP protocol-2	$KMnO_4$, Cysteine, Methionine	2-7	-	80
MnO_2 NP protocol-3	$KMnO_4$, H_2O_2 and polyvinyl alcohol	50	-	81
SnO_2 NP protocol-1	$SnCl_2$, thiourea	3	-	82
SnO_2 NP protocol-2	$SnCl_4 \cdot 5H_2O$, PEG, CTAB, SHMP	4	-	83
SnO_2 NP protocol-3	Sn- isopropoxide, Acetylacetone, p-toluenesulfonic acid	2	weeks	84

Among the metal oxides NPs, here we demonstrate the protocol for Fe_3O_4, TiO_2, MnO_2, SnO_2, CuO. Fe_3O_4 NPs were prepared from the reaction of mixed oxidation state salts of $Fe^{2+/}Fe^{3+}$ and citric acid just by magnetic stirring at 65° C for 10 minutes. In another method, Fe_3O_4 NPs with a scale of 12 nm were prepared by the reaction of $FeCl_2$ and dodecylamine by simple stirring at 85 ^oC. In the third protocol, Iron (III) acetylacetonate was refluxed in 2-pyrrolidone, and 5 nm scale Fe_3O_4 NPs were produced within 10 minutes. TiO_2 nanoparticles were synthesized from the reaction of $TiCl_4$, oleylamine, and 2,3-dimercaptosuccinic acid by refluxing at 270 ^oC for 10 minutes. By autoclave heating at 150 °C for 10 h, Tetra-n-butyl titanate and polyethylene glycol-400, produced water-soluble TiO_2 nanoparticles. Titanium n butoxide reacts with different molecular weights of PEG at 150^o C for 5 h in an autoclave and produces longstanding water-soluble titanium oxide nanoparticles.

CuO nanoparticles were synthesized from the reaction of tetraoctylammonium bromide, $CuSO_4.5H_2O$, and NaOH by gentle shaking and 85 °C temperature heating for 15 minutes. In other methods, CuO nanoparticles were synthesized from the reaction among Triton X-100, $CuCl_2$, and NaOH with 3 hours waiting at room temperature. Using a microemulsion of dioctylsulfosuccinate sodium salt and isooctane, $CuCl_2$ converts to CuO in an alkaline medium within 3 hours. MnO_2 colloidal NPs are prepared from the reduction of $KMnO_4$ with different types of reducing agents - manganese sulfate ($MnSO_4$), formic acid (HCO_2H), and sodium thiosulfate ($Na_2S_2O_3$) by simple stirring at room temperature. The reduction of $KMnO_4$ by Cysteine and Methionine produces MnO_2 colloidal NPs within 2-3 minutes.

According to another protocol of MnO_2 nanoparticles synthesis, using mixed reducing agent hydrogen peroxide and polyvinyl alcohol, $KMnO_4$ is converted to MnO_2. Thiourea-capped colloidal SnO_2 NPs were prepared from the reaction of stannous dichloride in an aqueous medium. Around 4 nm scale SnO_2 stabilized by PEG, CTAB, and SHMP are prepared from the reaction of any of the polymers and $SnCl_4$ in an alkaline medium by incubation at 160 ^oC for 12 hours. By the reaction of tin isopropoxide and acetylacetone in ethanol, SnO_2 NPs are made in 24 hours at 60 ^oC.

Conclusion

In brief, agarwood is one of the most expensive forestry products in the world. Our plan is to produce this valuable agarwood throughout the entire tree by nanoparticle inoculation. For this purpose, we have compiled various synthetic protocols for water-dispersible metal and metal oxide nanoparticles. First, we explain the basic principles of different types of wet chemical methods for nanoparticles synthesis. These include the growth mechanism of nanoparticles, the basic principle of synthesizing metals/metal oxides from aqueous solutions, the reduction process of metals, nucleation, growth mechanism, size and shape controlling mechanism, microwave heating-assisted wet chemical processes, ultra-sonication processes of nanoparticles synthesis, sol-gel chemistry of aqueous metal/metal oxides, common selection criteria of surfactants, microemulsion methods for metals/metal oxides nanoparticles synthesis, and surface functionalization mechanisms of nanoparticles.

Later, we focused on direct synthesis protocols for metal/metal oxides nanoparticles. We compiled at least three protocols for each species of nanoparticles. In this review, we discussed four noble metals and five metal oxide nanoparticles synthesis protocols. These include Silver (Ag), Gold, Platinum (Pt), and Palladium (Pd). The metal oxides are Fe_3O_4, TiO_2, MnO_2, SnO_2, CuO.

All the protocols are suitable for water-dispersible colloidal nanoparticle synthesis. This compiled information will help researchers to find an easy route for nanoparticle synthesis and application in biotechnology. Here, we believe these

protocols will enable the production of cell-permeable, sized, and stable nanoparticles in an aqueous medium for agarwood inoculation.

5. Acknowledgment

This work is supported by the Government of Bangladesh (GOB) fund, under the project "Whole Tree Agarwood Inoculation Project," (project code 224350400) at the Bangladesh Forest Research Institute (BFRI), an organization of the Ministry of Environment, Forest and Climate Change, Republic of Bangladesh.

6. Conflict of Interest

The authors declare no conflict of interest at any point during the research.

References

Abid, N., Khan, A. M., Shujait, S., Chaudhary, K., Ikram, M., Imran, M., ... & Maqbool, M. (2022). Synthesis of nanomaterials using various top-down and bottom-up approaches, influencing factors, advantages, and disadvantages: A review. *Advances in Colloid and Interface Science*, *300*, 102597.

Agnoli, F., Zhou, W. L., & O'Connor, C. J. (2001). Synthesis of Cubic Antiferromagnetic KMnF3 Nanoparticles Using Reverse Micelles and Their Self-Assembly. *Advanced Materials*, *13*(22), 1697-1699.

Akhtar, S., Shahzad, K., Mushtaq, S., Ali, I., Rafe, M. H., & Fazal-ul-Karim, S. M. (2019). Antibacterial and antiviral potential of colloidal Titanium dioxide (TiO2) nanoparticles suitable for biological applications. *Materials Research Express*, *6*(10), 105409.

Ali, K., Saquib, Q., Ahmed, B., Siddiqui, M. A., Ahmad, J., Al-Shaeri, M., ... & Musarrat, J. (2020). Bio-functionalized CuO nanoparticles induced apoptotic activities in human breast carcinoma cells and toxicity against Aspergillus flavus: an in vitro approach. *Process Biochemistry*, *91*, 387-397.

Amendola, V., Pilot, R., Frasconi, M., Maragò, O. M., &Iatì, M. A. (2017). Surface plasmon resonance in gold nanoparticles: a review. *Journal of Physics: Condensed Matter*, *29*(20), 203002.

Atha, D. H., Wang, H., Petersen, E. J., Cleveland, D., Holbrook, R. D., Jaruga, P., ... & Nelson, B. C. (2012). Copper oxide nanoparticle mediated DNA damage in terrestrial plant models. *Environmental science & technology*, *46*(3), 1819-1827.

Aslam, M., Schultz, E. A., Sun, T., Meade, T., & Dravid, V. P. (2007). Synthesis of amine-stabilized aqueous colloidal iron oxide nanoparticles. *Crystal growth & design*, *7*(3), 471-475.

Barrena, R., Casals, E., Colón, J., Font, X., Sánchez, A., & Puntes, V. (2009). Evaluation of the ecotoxicity of model nanoparticles. *Chemosphere*, *75*(7), 850-857.

Battke, F., Leopold, K., Maier, M., Schmidhalter, U., & Schuster, M. (2008). Palladium exposure of barley: uptake and effects. *Plant biology*, *10*(2), 272-276.

Bhatia, S. (2016). *Natural polymer drug delivery systems: Nanoparticles, plants, and algae*. Springer.

Bigall, N. C., Härtling, T., Klose, M., Simon, P., Eng, L. M., & Eychmüller, A. (2008). Monodisperse platinum nanospheres with adjustable diameters from 10 to 100 nm: synthesis and distinct optical properties. *Nano letters*, *8*(12), 4588-4592.

Blanchette, R. A., & Chowdhury, S. M. (2009). *Introduction of New Technology for Sustainable Agarwood Production in Bangladesh*. Sher-e-Bangia Agricultural University Research System (SAURES).

Bönnemann, H., Braun, G., Brijoux, W., Brinkmann, R., Tilling, A. S., Seevogel, K., & Siepen, K. (1996). Nanoscale colloidal metals and alloys stabilized by solvents and surfactants Preparation and use as catalyst precursors. *Journal of Organometallic Chemistry*, *520*(1-2), 143-162.

Boutonnet, M., Kizling, J., Stenius, P., & Maire, G. (1982). The preparation of monodisperse colloidal metal particles from microemulsions. *Colloids and surfaces*, *5*(3), 209-225.

Boykov, I. N., Shuford, E., & Zhang, B. (2019). Nanoparticle titanium dioxide affects the growth and microRNA expression of switchgrass (Panicum virgatum). *Genomics*, *111*(3), 450-456.

Cao, Y., Hu, J. C., Hong, Z. S., Deng, J. F., & Fan, K. N. (2002). Characterization of high-surface-area zirconia aerogel synthesized from combined alcohothermal and supercritical fluid drying techniques. *Catalysis letters*, *81*, 107-112.

Ciacchi, L. C., Mertig, M., Pompe, W., Meriani, S., & Alessandro, D. V. (2003). Nucleation and growth of platinum clusters in solution and on biopolymers. *Platinum Metals Review*, *47*(3), 98-107.

Cushing, B. L., Kolesnichenko, V. L., & O'connor, C. J. (2004). Recent advances in the liquid-phase syntheses of inorganic nanoparticles. *Chemical reviews*, *104*(9), 3893-3946.

de Monredon, S., Cellot, A., Ribot, F., Sanchez, C., Armelao, L., Gueneau, L., & Delattre, L. (2002). Synthesis and characterization of crystalline tin oxide nanoparticles. *Journal of Materials Chemistry*, *12*(8), 2396-2400.

Dheyab, M. A., Aziz, A. A., Jameel, M. S., Noqta, O. A., Khaniabadi, P. M., & Mehrdel, B. (2020). Simple rapid stabilization method through citric acid modification for magnetite nanoparticles. *Scientific reports*, *10*(1), 10793.

Diao, Y., Walawender, W. P., Sorensen, C. M., Klabunde, K. J., & Ricker, T. (2002). Hydrolysis of magnesium methoxide. Effects of toluene on gel structure and gel chemistry. *Chemistry of materials*, *14*(1), 362-368.

Doty, R. C., Tshikhudo, T. R., Brust, M., &Fernig, D. G. (2005). Extremely stable water-soluble Ag nanoparticles. *Chemistry of Materials*, *17*(18), 4630-4635.

Elaissari, A. (Ed.). (2008). *Colloidal nanoparticles in biotechnology*. John Wiley & Sons.

Gao, M., Han, X., Sun, Y., Chen, H., Yang, Y., Liu, Y., ... & Han, J. (2019). Overview of sesquiterpenes and chromones of agarwood originating from four main species of the genus Aquilaria. *RSC advances*, *9*(8), 4113-4130.

Hill, A. E. (1994). Osmotic flow in membrane pores of molecular size. *The Journal of Membrane Biology*, *137*, 197-203.

Hossain, J. et al. (2020). Nanotechnology for High Quality Agarwood Resin Formation. *International Journal of Business, Social and Scientific Research. 9*(1), 18–25.

Hossain, M. N., Chowdhury, M. H., Islam, M. J., & Akhter, T. S. (2013). Analysis of the properties of ZnO nanoparticle for emerging applications in nanoscale domains. In *2013 IEEE 56th International Midwest Symposium on Circuits and Systems (MWSCAS) (pp. 928-931), IEEE*.

Islam, M. A., & Rahman, M. M. (2013). Soluble colloidal manganese dioxide: formation, identification and prospects of application. *Colloid Journal*, *75*, 538-542.

Khan, M. R., Adam, V., Rizvi, T. F., Zhang, B., Ahamad, F., Jośko, I., ... & Mao, C. (2019). Nanoparticle–plant interactions: two-way traffic. *Small*, *15*(37), 1901794.

Khan, Z., Al-Thabaiti, S. A., Obaid, A. Y., & Khan, Z. A. (2010). MnO_2 nanostructures of different morphologies from amino acids–MnO_4^- reactions in aqueous solutions. *Colloids and Surfaces B: Biointerfaces*, *81*(1), 381-384.

Kumar, A., Kuang, Y., Liang, Z., & Sun, X. (2020). Microwave chemistry, recent advancements, and eco-friendly microwave-assisted synthesis of nanoarchitectures and their applications: A review. *Materials Today Nano*, *11*, 100076.

Lai, W. Y., Feng, S. W., Chan, Y. H., Chang, W. J., Wang, H. T., & Huang, H. M. (2018). In vivo investigation into effectiveness of Fe3O4/PLLA nanofibers for bone tissue engineering applications. *Polymers*, *10*(7), 804.

LaMer, V. K., & Dinegar, R. H. (1950). Theory, production and mechanism of formation of monodispersed hydrosols. *Journal of the american chemical society*, *72*(11), 4847-4854.

Landa, P. (2021). Positive effects of metallic nanoparticles on plants: Overview of involved mechanisms. *Plant Physiology and Biochemistry*, *161*, 12-24.

Le, T. H., Ngo, T. H. A., Doan, V. T., Nguyen, L. M. T., & Le, M. C. (2019). Preparation of manganese dioxide nanoparticles on laterite for methylene blue degradation. *Journal of Chemistry*, *2019*.

Li, G., Zeng, C., & Jin, R. (2015). Chemoselective hydrogenation of nitrobenzaldehyde to nitrobenzyl alcohol with unsupported Au nanorod catalysts in water. *The Journal of Physical Chemistry C*, *119*(20), 11143-11147.

Li, J., Hu, J., Ma, C., Wang, Y., Wu, C., Huang, J., & Xing, B. (2016). Uptake, translocation and physiological effects of magnetic iron oxide (γ-Fe2O3) nanoparticles in corn (Zea mays L.). *Chemosphere*, *159*, 326-334.

Li, Y., Kröger, M., & Liu, W. K. (2012). Nanoparticle geometrical effect on structure, dynamics and anisotropic viscosity of polyethylene nanocomposites. *Macromolecules*, *45*(4), 2099-2112.

Li, Z., Chen, H., Bao, H., & Gao, M. (2004). One-pot reaction to synthesize water-soluble magnetite nanocrystals. *Chemistry of Materials*, *16*(8), 1391-1393.

Lin, D., & Xing, B. (2008). Root uptake and phytotoxicity of ZnO nanoparticles. *Environmental science & technology*, *42*(15), 5580-5585.

Liu, Y., Chen, H., Yang, Y., Zhang, Z., Wei, J., Meng, H., ... & Chen, H. (2013). Whole-tree agarwood-inducing technique: an efficient novel technique for producing high-quality agarwood in cultivated Aquilaria sinensis trees. *Molecules*, *18*(3), 3086-3106.

Logothetidis, S., (2011). Nanotechnology: Principles and applications. In *Nanostructuredmaterials and their applications* (pp. 1-22). Berlin, Heidelberg: Springer Berlin Heidelberg.

Lu, X., Wang, H., Wang, Z., Jiang, Y., Cao, D., & Yang, G. (2016). Room-temperature synthesis of colloidal SnO_2 quantum dot solution and ex-situ deposition on carbon nanotubes as anode materials for lithium ion batteries. *Journal of Alloys and Compounds*, *680*, 109-115.

Malik, M. A., Wani, M. Y., & Hashim, M. A. (2012). Microemulsion method: A novel route to synthesize organic and inorganic nanomaterials: 1st Nano Update. *Arabian journal of Chemistry*, *5*(4), 397-417.

Matsui, I. (2005). Nanoparticles for electronic device applications: a brief review. *Journal of Chemical Engineering of Japan*, *38*(8), 535-546.

McNeil, P. L. (1984). Mechanisms of nutritive endocytosis. III. A freeze-fracture study of phagocytosis by digestive cells of Chlorohydra. *Tissue and Cell*, *16*(4), 519-533.

Mendis, P., de Silva, R. M., de Silva, K. N., Wijenayaka, L. A., Jayawardana, K., & Yan, M. (2016). Nanosilver rainbow: a rapid and facile method to tune different colours of nanosilver through the controlled synthesis of stable spherical silver nanoparticles. *RSC advances*, *6*(54), 48792-48799.

Monopoli, A., Calo, V., Ciminale, F., Cotugno, P., Angelici, C., Cioffi, N., & Nacci, A. (2010). Glucose as a clean and renewable reductant in the Pd-nanoparticle-catalyzed reductive homocoupling of bromo-and chloroarenes in water. *The Journal of Organic Chemistry*, *75*(11), 3908-3911.

Nandanwar, S. U., & Chakraborty, M. (2012). Synthesis of colloidal CuO/γ-Al_2O_3 by microemulsion and its catalytic reduction of aromatic nitro compounds. *Chinese Journal of Catalysis*, *33*(9-10), 1532-1541.

Nassar, N. N., & Husein, M. M. (2007). Effect of microemulsion variables on copper oxide nanoparticle uptake by AOT microemulsions. *Journal of colloid and interface science*, *316*(2), 442-450.

Nurakhmetova, Z. A., Azhkeyeva, A. N., Klassen, I. A., &Tatykhanova, G. S. (2020). Synthesis and stabilization of gold nanoparticles using water-soluble synthetic and natural polymers. *Polymers*, *12*(11), 2625.

Oskam, G. (2006). Metal oxide nanoparticles: synthesis, characterization and application. *Journal of sol-gel science and technology*, *37*, 161-164.

Parashar, M., Shukla, V. K., & Singh, R. (2020). Metal oxides nanoparticles via sol–gel method: a review on synthesis, characterization and applications. *Journal of Materials Science: Materials in Electronics*, *31*, 3729-3749.

Pastoriza-Santos, I., & Liz-Marzán, L. M. (2002). Formation of PVP-protected metal nanoparticles in DMF. *Langmuir*, *18*(7), 2888-2894.

Pérez-de-Luque, A. (2017). Interaction of nanomaterials with plants: what do we need for real applications in agriculture? *Frontiers in Environmental Science*, *5*, 12.

Prasad, P., Gordijo, C. R., Abbasi, A. Z., Maeda, A., Ip, A., Rauth, A. M., ... & Wu, X. Y. (2014). Multifunctional albumin–MnO2 nanoparticles modulate solid tumor microenvironment by attenuating hypoxia, acidosis, vascular endothelial growth factor and enhance radiation response. *ACS nano*, *8*(4), 3202-3212.

Rahman, M. S., Chakraborty, A., Mazumdar, S., Nandi, N. C., Bhuiyan, M. N. I., Alauddin, S. M., ... & Hossain, M. J. (2020). Effects of poly (vinylpyrrolidone) protected platinum nanoparticles on seed germination and growth performance of Pisum sativum. *Nano-Structures & Nano-Objects*, *21*, 100408.

Rahmawati, M., Mahfud, C., Risuleo, G., & Jadid, N. (2022). Nanotechnology in plant metabolite improvement and in animal welfare. *Applied Sciences*, *12*(2), 838.

Raveendran, P., Fu, J., & Wallen, S. L. (2006). A simple and "green" method for the synthesis of Au, Ag, and Au–Ag alloy nanoparticles. *Green Chemistry*, *8*(1), 34-38.

Samsoon, S., Azam, M., Khan, A., Ashraf, M., Bhatti, H. N., Alshawwa, S. Z., & Iqbal, M. (2022). Green-synthesized MnO2 nanofertilizer impact on growth, photosynthetic pigment, and non-enzymatic antioxidant of Vigna unguiculata cultivar. *Biomass Conversion and Biorefinery*, 1-10.

Seo, J. W., Chung, H., Kim, M. Y., Lee, J., Choi, I. H., & Cheon, J. (2007). Development of water-soluble single-crystalline TiO2 nanoparticles for photocatalytic cancer-cell treatment. *Small*, *3*(5), 850-853.

Swanson, J. A. (2008). Shaping cups into phagosomes and macropinosomes. *Nature reviews Molecular cell biology*, *9*(8), 639-649.

Suslick, K. S., Choe, S. B., Cichowlas, A. A., & Grinstaff, M. W. (1991). Sonochemical synthesis of amorphous iron. *nature*, *353*(6343), 414-416.

Suslick, K. S., Fang, M., & Hyeon, T. (1996). Sonochemical synthesis of iron colloids. *Journal of the American Chemical Society*, *118*(47), 11960-11961.

Suthakaran, S., Dhanapandian, S., Krishnakumar, N., &Ponpandian, N. (2019). Surfactants assisted SnO_2 nanoparticles synthesized by a hydrothermal approach and potential applications in water purification and energy conversion. *Journal of Materials Science: Materials in Electronics*, *30*, 13174-13190.

Tan, C. S., Isa, N. M., Ismail, I., & Zainal, Z. (2019). Agarwood induction: current developments and future perspectives. *Frontiers in plant science*, *10*, 122.

Tan, Y., Dai, X., Li, Y., & Zhu, D. (2003). Preparation of gold, platinum, palladium and silver nanoparticles by the reduction of their salts with a weak reductant–potassium bitartrate. *Journal of Materials Chemistry*, *13*(5), 1069-1075.

Thompson, I. D., Lim, T., & Turjaman, M. (2022, November). Expensive, Exploited and Endangered—A Review of the Agarwood-Producing Genera Aquilaria and Gyrinops: CITES Considerations, Trade Patterns, Conservation, and Management. In *Proceedings of the Nineteenth Meeting of the Conference of the Parties, Panama City, Panama* (pp. 14-25).

Titus, D., Samuel, E. J., & Roopan, S. M. (2019). Green Synthesis, Characterization and Applications of Nanoparticles. *Micro and Nano Technologies*, *12*, 303-319.

Turkevich, J., Stevenson, P. C., & Hillier, J. (1951). A study of the nucleation and growth processes in the synthesis of colloidal gold. *Discussions of the Faraday Society*, *11*, 55-75.

Vittori Antisari, L., Carbone, S., Gatti, A., Vianello, G., &Nannipieri, P. (2015). Uptake and translocation of metals and nutrients in tomato grown in soil polluted with metal oxide (CeO_2, Fe_3O_4, SnO_2, TiO_2) or metallic (Ag, Co, Ni) engineered nanoparticles. *Environmental Science and Pollution Research* 22.3, 1841-1853.

Wei, J., Yang, Y., Zhang, Z., Meng, M., Feng, J., & Gan, B. (2010). Liquid infusion method for producing linaloe on Aquilaria sinensis tree. *CN101755629. State Intellectual Property office of the PRC, Beijing*, 1-5.

West, J. L., & Halas, N. J. (2000). Applications of nanotechnology to biotechnology: Commentary. *Current opinion in Biotechnology*, *11*(2), 215-217.

Wu, Q., Cao, H., Luan, Q., Zhang, J., Wang, Z., Warner, J. H., & Watt, A. R. (2008). Biomolecule-assisted synthesis of water-soluble silver nanoparticles and their biomedical applications. *Inorganic chemistry*, *47*(13), 5882-5888.

Wu, Z., Liu, W., Li, J., Yu, L., & Lin, L. (2020). Dynamic analysis of gene expression and determination of chemicals in agarwood in Aquilaria sinensis. *Journal of Forestry Research*, *31*(5), 1833-1841.

Wyman, C. E. (Ed.). (2013). *Aqueous pretreatment of plant biomass for biological and chemical conversion to fuels and chemicals*. John Wiley & Sons.

Xia, Y., Xiong, Y., Lim, B., & Skrabalak, S. E. (2009). Shape-controlled synthesis of metal nanocrystals: simple chemistry meets complex physics?. *Angewandte Chemie International Edition*, *48*(1), 60-103.

Xiong, Y., Cai, H., Wiley, B. J., Wang, J., Kim, M. J., & Xia, Y. (2007). Synthesis and mechanistic study of palladium nanobars and nanorods. *Journal of the American Chemical Society*, *129*(12), 3665-3675.

Xu, S., & Yang, Q. (2008). Well-dispersed water-soluble Pd nanocrystals: Facile reducing synthesis and application in catalyzing organic reactions in aqueous media. *The Journal of Physical Chemistry C*, *112*(35), 13419-13425.

Yaqoob, S. B., Adnan, R., Rameez Khan, R. M., & Rashid, M. (2020). Gold, silver, and palladium nanoparticles: a chemical tool for biomedical applications. *Frontiers in Chemistry*, *8*, 376.

Yan, X., Pan, D., Li, Z., Liu, Y., Zhang, J., Xu, G., & Wu, M. (2010). Controllable synthesis and photocatalytic activities of water-soluble TiO2 nanoparticles. *Materials Letters*, *64*(16), 1833-1835.

Yin, L., Colman, B. P., McGill, B. M., Wright, J. P., & Bernhardt, E. S. (2012). Effects of silver nanoparticle exposure on germination and early growth of eleven wetland plants. e47674.

Yonezawa, T., Sutoh, M., & Kunitake, T. (1997). Practical preparation of size-controlled gold nanoparticles in water. *Chemistry letters*, *26*(7), 619-620.

Yonezawa, T., Onoue, S. Y., & Kimizuka, N. (2000). Preparation of highly positively charged silver nanoballs and their stability. *Langmuir*, *16*(12), 5218-5220.

Zhang, L. N., Deng, H. H., Lin, F. L., Xu, X. W., Weng, S. H., Liu, A. L., ... & Chen, W. (2014). In situ growth of porous platinum nanoparticles on graphene oxide for colorimetric detection of cancer cells. *Analytical chemistry*, *86*(5), 2711-2718.

Zhang, M., Lei, J., Shi, Y., Zhang, L., Ye, Y., Li, D., & Mu, C. (2016). Molecular weight effects of PEG on the crystal structure and photocatalytic activities of PEG-capped TiO 2 nanoparticles. *RSC advances*, *6*(86), 83366-83372.

Zhang, S., Gao, H., & Bao, G. (2015). Physical principles of nanoparticle cellular endocytosis. *ACS nano*, *9*(9), 8655-8671. (b). Decuzzi, P., & Ferrari, M. (2007). The role of specific and non-specific interactions in receptor-mediated endocytosis of nanoparticles. *Biomaterials*, *28*(18), 2915-2922.